mathematics

MDPI

Article

Global Well-Posedness and Stability of Nonlocal Damage-Structured Lineage Model with Feedback and Dedifferentiation

Ye Liang [1,†], Louis Shuo Wang [2,†], Jiguang Yu [1,3,*,†] and Zonghao Liu [4,*]

[1] Department of Mathematics, University College London, London WC1E 6BT, UK; zcahiad@ucl.ac.uk
[2] Department of Mathematics, University of Tennessee, Knoxville, TN 37996, USA; swang116@vols.utk.edu
[3] College of Engineering, Boston University, Boston, MA 02215, USA
[4] Innovation Center for Cancer Research, Clinical Oncology School, Fujian Medical University, Fuzhou 350014, China
* Correspondence: zcahyuc@ucl.ac.uk (J.Y.); liuzonghao@fjmu.edu.cn (Z.L.)
† These authors contributed equally to this work as co-first authors.

Abstract

A nonlocal transport–reaction system is proposed to model the coupled dynamics of stem and differentiated cell populations, structured by a continuous damage variable. The framework incorporates bidirectional transitions via differentiation and dedifferentiation, with nonlocal birth operators encoding damage redistribution upon division and Hill-type feedback regulation dependent on total populations. Global well-posedness of solutions in $C([0,\infty); L^1([0,\infty) \times L^1([0,\infty)))$ is established by combining the contraction mapping principle for local existence with a priori L^1 bounds for global existence, ensuring uniqueness and nonnegativity. Integration yields balance laws for total populations, reducing to a finite-dimensional autonomous ordinary differential equation (ODE) system under constant death rates. Linearization reveals a bifurcation threshold separating extinction, homeostasis, and unbounded growth. Under compensatory feedback, Dulac's criterion precludes periodic orbits, and the Poincaré–Bendixson theorem confines bounded trajectories to equilibria or heteroclinics. Uniqueness implies global asymptotic stability. A scaling invariance for steady states under uniform feedback rescaling is identified. The analysis extends structured population theory to feedback-regulated compartments with nonlocal operators and reversible dedifferentiation, providing explicit stability criteria and linking an infinite-dimensional structured model to tractable low-dimensional reductions.

Keywords: structured population model; global well-posedness; dedifferentiation; bifurcation and global stability

MSC: 34D23; 35L60; 35Q49; 35Q92; 37N25; 92C37

check for updates

Academic Editor: Necibe Tuncer

Received: 17 October 2025
Revised: 1 November 2025
Accepted: 6 November 2025
Published: 7 November 2025

Citation: Liang, Y.; Wang, L.S.; Yu, J.; Liu, Z. Global Well-Posedness and Stability of Nonlocal Damage-Structured Lineage Model with Feedback and Dedifferentiation. *Mathematics* **2025**, *13*, 3583. https://doi.org/10.3390/math13223583

Copyright: © 2025 by the authors. Licensee MDPI, Basel, Switzerland. This article is an open access article distributed under the terms and conditions of the Creative Commons Attribution (CC BY) license (https://creativecommons.org/licenses/by/4.0/).

1. Introduction

Stem cells maintain tissue homeostasis by producing progenitors and terminally differentiated (TD) cells to keep a hierarchical differentiation structure within the stem cell lineage [1–5]. Certain feedback loops exist in lineages for tissue maintenance and robust response to environmental changes [6–9]. On the other hand, recent advances in cell biology demonstrate that differentiation is not strictly irreversible, and TD cells may revert to a stem-like stage through dedifferentiation [10–14]. This plasticity contributes to tissue regeneration but also underlies oncogenic transformations and therapeutic resistance [15–19].

Moreover, stem cell aging, driven by the progressive accumulation of cellular damage, disrupts homeostatic balance and elevates malignancy risks [20–24].

Motivated by these phenomena, a compact transport–reaction model for stem P and TD W cell densities structured by a continuous damage variable $x \geq 0$ is proposed. The model incorporates advective damage accumulation, nonlocal birth operators that redistribute damage at division, reversible dedifferentiation $W \to P$, and Hill-type feedback that modulate division and transition rates. The model reads

$$\begin{cases} \partial_t P + v_P \partial_x P = \mathcal{B}_P[P](t,x) - \lambda_P P(t,x) + \lambda_R W(t,x), & x > 0,\ t > 0, \\ \partial_t W + v_W \partial_x W = \mathcal{B}_W[P](t,x) - (\delta(x) + \lambda_R) W(t,x), & x > 0,\ t > 0, \\ P(t,0) = W(t,0) = 0, & t \geq 0, \\ P(0,x) = P_0(x),\ W(0,x) = W_0(x), & x > 0. \end{cases} \tag{1}$$

Here, $v_P, v_W > 0$ denote the rates of damage accumulation, $\lambda_P \geq 0$ is the proliferation rate of stem cells, $\lambda_R \geq 0$ the dedifferentiation rate, and $\delta(x) \geq 0$ the death rate of TD cells. The nonlocal birth operators $\mathcal{B}_P$ and $\mathcal{B}_W$ describe self-renewal and differentiation processes with redistribution of damage following cell division. The structure of Equation (1) combines transport along the damage axis with nonlocal division terms. This model builds on the foundational theory of transport equations and structured partial differential equations (PDEs) [25,26] and extends prior frameworks by introducing a damage variable linked to stem and TD compartments, dedifferentiation fluxes, and nonlinear feedback regulation [27–30].

Numerous mathematical models have been proposed to investigate the process of dedifferentiation, as highlighted by various studies [31]. These works examine their impact on tumor growth and treatment response [32], stochastic and evolutionary dynamics [33–35], mutation accumulation and cancer initiation [36], transient dynamics and tumor invasion [37–40], and therapy resistance [41]. Apart from dedifferentiation, the continuum model of stem cell aging [42] describes two damage- and cycle-structured hyperbolic PDEs with nonlocal division and Hill-type feedback. It assumes irreversible differentiation and is analyzed numerically without rigorous well-posedness or global stability results.

Unlike parabolic frameworks, our system is first-order hyperbolic and describes advective transport of the damage variable. The analysis establishes global well-posedness in $C([0,\infty); L^1 \times L^1)$, derives balance laws, and obtains an exact reduction to a two-dimensional autonomous ODE under constant TD mortality. Analysis of the reduced system yields an explicit bifurcation threshold separating extinction, homeostasis, and unbounded growth, a global nonoscillation result (Dulac), and, under compensatory feedback, global asymptotic stability (Poincaré–Bendixson).

The paper is organized as follows. Section 2 establishes global well-posedness of solutions to the PDE system, including existence, uniqueness, and positivity. Section 3 derives the reduced ODE system for total populations. Sections 4 and 5 provide, respectively, local and global stability analyses of equilibria. Section 6 presents numerical illustrations supporting analytical results. The concluding section discusses biological implications, model limitations, and future extensions.

2. PDE Model and Well-Posedness

The transport–reaction system is studied in $C([0,\infty); L^1([0,\infty)) \times L^1([0,\infty)))$. The analysis starts with the explicit partition operators and then develops the functional–analytic framework.

The construction of the nonlocal birth operators in Equation (1) is now outlined. Stem-cell division is modeled as a renewal process where the damage of a mother cell is

partitioned between its daughters, inducing a nonlocal dependence on the damage variable. Let $P(t,x')$ be the density of stem cells with damage x', dividing at rate λ_P. Each division follows one of three modes with probabilities p_1, p_2, p_3 (symmetric self-renewal, symmetric differentiation, and asymmetric division, respectively; $p_1+p_2+p_3=1$). Only stem cells divide, so the birth terms depend on P.

If a daughter inherits a fraction $\theta \in (0,1)$ of the mother's damage, its damage satisfies $x=\theta x'$. Let $K_{(\cdot)}(x,x')$ be the probability density that a daughter with damage x arises from a mother with damage x'. Summing the daughter flux with damage level x from the mother cell with damage level x' over all possible mother cell damage levels x' yields the total daughter flux

$$\int_0^\infty \lambda_P\, p_i\, K_{i,(\cdot)}(x,x')\, P(t,x')\, dx'.$$

Two stem daughters inherit damage fractions α_1, α_2 in symmetric self-renewal, two TD daughters inherit β_1, β_2 in symmetric differentiation, and the stem daughter inherits γ_1, with the TD daughter inheriting γ_2 in asymmetric division. The fractions satisfy

$$\alpha_1+\alpha_2=\beta_1+\beta_2=\gamma_1+\gamma_2=1, \quad \min\{\alpha_i,\beta_i,\gamma_i\}>0,$$

and the delta kernels take the form [43]

$$\begin{aligned} K_{1,P}(x,x') &= \delta(x-\alpha_1 x') + \delta(x-\alpha_2 x'),\\ K_{2,W}(x,x') &= \delta(x-\beta_1 x') + \delta(x-\beta_2 x'),\\ K_{3,P}(x,x') &= \delta(x-\gamma_1 x'),\\ K_{3,W}(x,x') &= \delta(x-\gamma_2 x'). \end{aligned}$$

Incorporating three stem cell division modes with their probabilities and damage partition parameters, the birth operator is taken as

$$\begin{aligned} \mathcal{B}_P[P](t,x) &:= \int_0^\infty p_1\lambda_P K_{1,P}(x,x')P(t,x')\,dx' + \int_0^\infty p_3\lambda_P K_{3,P}(x,x')P(t,x')\,dx',\\ \mathcal{B}_W[P](t,x) &:= \int_0^\infty p_2\lambda_P K_{2,W}(x,x')P(t,x')\,dx' + \int_0^\infty p_3\lambda_P K_{3,W}(x,x')P(t,x')\,dx'. \end{aligned}$$

Substituting these kernels into the integral expressions above and using the scaling property of the Dirac delta,

$$\delta(\alpha x) = \frac{1}{|\alpha|}\delta(x), \qquad \alpha \neq 0,$$

one obtains

$$\int_0^\infty p_i\lambda_P K(x,x')P(t,x')\,dx' = \int_0^\infty p_i\lambda_P \delta(x-\alpha x')P(t,x')\,dx' = \frac{p_i\lambda_P}{\alpha}P(t,x/\alpha).$$

Collecting all division modes yields the explicit nonlocal advection–reaction system

$$\begin{cases} \partial_t P + v_P\partial_x P = \frac{p_1\lambda_P}{\alpha_1}P(t,x/\alpha_1) + \frac{p_1\lambda_P}{\alpha_2}P(t,x/\alpha_2) + \frac{p_3\lambda_P}{\gamma_1}P(t,x/\gamma_1) - \lambda_P P + \lambda_R W, & x>0,\ t>0,\\ \partial_t W + v_W\partial_x W = \frac{p_2\lambda_P}{\beta_1}P(t,x/\beta_1) + \frac{p_2\lambda_P}{\beta_2}P(t,x/\beta_2) + \frac{p_3\lambda_P}{\gamma_2}P(t,x/\gamma_2) - (\delta(x)+\lambda_R)W, & x>0,\ t>0,\\ P(t,0)=W(t,0)=0, & t\geq 0,\\ P(0,x)=P_0(x),\ W(0,x)=W_0(x), & x>0. \end{cases} \tag{2}$$

The initial data $P_0(x), W_0(x)$ are nonnegative and belong to $L^1([0,\infty))$.

Feedback is encoded using Hill-type laws that depend on the totals

$$\bar{P}(t) := \int_0^\infty P(t,x)\,dx, \quad \bar{W}(t) := \int_0^\infty W(t,x)\,dx.$$

The maps

$$p_1(t) = \frac{\hat{p}_1}{1+(k_1\bar{W}(t))^{m_1}}, \tag{3}$$

$$p_2(t) = \frac{\hat{p}_2}{1+(k_2\bar{W}(t))^{m_2}}, \tag{4}$$

$$\lambda_P(t) = \frac{\hat{\lambda}_P}{1+(k_3\bar{W}(t))^{m_3}}, \tag{5}$$

$$\lambda_R(t) = \frac{\hat{\lambda}_R}{1+(k_4\bar{P}(t))^{m_4}}, \tag{6}$$

use baseline values $\hat{p}_1$, $\hat{p}_2$, $\hat{\lambda}_P$, $\hat{\lambda}_R$, strength $k_i > 0$, and exponents $m_i \geq 1$. The renewal fraction f is introduced to represent the effective probability that a proliferating stem cell self-renews rather than differentiates at time t. Biologically, $f(t) \in [0,1]$ quantifies the balance between symmetric self-renewal p_1 and differentiation p_2, with $2f(t) - 1 = p_1(t) - p_2(t)$ measuring the net bias toward renewal. When $k_1 = k_2$ and $m_1 = m_2$, the renewal fraction satisfies

$$2f(t) - 1 = p_1(t) - p_2(t) = \frac{2\hat{f} - 1}{1+(k_1\bar{W}(t))^{m_1}}, \quad \hat{f} = \frac{1+\hat{p}_1-\hat{p}_2}{2}. \tag{7}$$

The baseline value $\hat{f}$ gives the renewal tendency in the absence of feedback ($\bar{W} = 0$).

2.1. Notation and Standing Assumptions

Write $\|\cdot\|$ for the $L^1([0,\infty))$ norm and $L^1_+([0,\infty))$ for the cone of almost-everywhere nonnegative functions. For $T > 0$ define

$$\mathcal{X}_T := C\Big([0,T]; L^1([0,\infty)) \times L^1([0,\infty))\Big), \quad \|(P,W)\|_{\mathcal{X}_T} := \sup_{0\leq t\leq T}(\|P(t,\cdot)\| + \|W(t,\cdot)\|).$$

and set $\mathcal{X}_\infty := C([0,\infty); L^1([0,\infty)) \times L^1([0,\infty)))$ with the analogous norm. The following hypotheses are adopted.

(H1) Fix p_i $(i = 1,2)$, λ_P, λ_R by Equations (3)–(6) with $k_i > 0$ and $m_i \geq 1$ for $i = 1,2,3,4$; the probabilities satisfy $p_1 + p_2 + p_3 = 1$; the fractions satisfy $\alpha_1 + \alpha_2 = \beta_1 + \beta_2 = \gamma_1 + \gamma_2 = 1$ with $\min\{\alpha_i, \beta_i, \gamma_i\} > 0$; the death rate $\delta(x)$ is nondecreasing, bounded, and equals a positive constant in the constant death case.

(H2) $P_0(x), W_0(x) \in L^1_+([0,\infty))$.

Define the nonlocal birth operators compactly as follows:

$$\begin{aligned}
\mathcal{B}_P[P](t,x) &:= \frac{p_1(t)\lambda_P(t)}{\alpha_1}P(t,x/\alpha_1) + \frac{p_1(t)\lambda_P(t)}{\alpha_2}P(t,x/\alpha_2) + \frac{p_3(t)\lambda_P(t)}{\gamma_1}P(t,x/\gamma_1),\\
\mathcal{B}_W[P](t,x) &:= \frac{p_2(t)\lambda_P(t)}{\beta_1}P(t,x/\beta_1) + \frac{p_2(t)\lambda_P(t)}{\beta_2}P(t,x/\beta_2) + \frac{p_3(t)\lambda_P(t)}{\gamma_2}P(t,x/\gamma_2).
\end{aligned} \tag{8}$$

Table 1 lists all notations in this work.

Table 1. Summary of main notation.

Symbol	Meaning
$\bar{P}(t) = \int_0^\infty P(t,x)\,dx$	Total stem-cell population at time t
$\bar{W}(t) = \int_0^\infty W(t,x)\,dx$	Total TD cell population at time t
$M(t) = \bar{P}(t) + \bar{W}(t)$	Total cell mass
v_P, v_W	Damage accumulation velocities in P and W compartments
$\mathcal{B}_P, \mathcal{B}_W$	Nonlocal birth operators (damage partitioning at division)
λ_P	Effective replication rate of P
λ_R	Dedifferentiation rate from W to P (possibly state dependent)
α_i, β_i, γ_i	Partition fractions in stem cell divisions
$\delta(x) \geq 0$	Death rate of W (damage dependent, or constant δ)
$\hat{p}_i$, $\hat{\lambda}_P$, $\hat{\lambda}_R$	Baseline (unregulated) probabilities and rates
$k_i > 0$	Feedback strength parameters in Hill-type regulation
$m_i \geq 1$	Hill exponents governing feedback steepness
$\mathcal{S} = (\bar{P}^*, \bar{W}^*)$	Equilibrium/steady state of the reduced ODE system

The nonlinear coefficients can be extended to globally Lipschitz functions.

Lemma 1. *(i) Globally Lipschitz extensions of the coefficients: The nonlinearities p_i $(i = 1,2,3)$, λ_P, and λ_R on $[0,\infty)$ can be extended to globally Lipschitz functions $\tilde{p}_i, \tilde{\lambda}_p, \tilde{\lambda}_R$ on $\mathbb{R}$ with the Lipschitz bounds $L_1, L_2, L_1 + L_2, L_3, L_4$ for $\tilde{p}_1, \tilde{p}_2, \tilde{p}_3, \tilde{\lambda}_P, \tilde{\lambda}_R$, respectively, where $L_1, L_2, L_3, L_4 > 0$ are positive constants.*

(ii) L^1 boundedness of $\mathcal{B}_P, \mathcal{B}_W$: Let $\mathcal{B}_P, \mathcal{B}_W$ be the nonlocal birth operators in (8). Then for all $t \geq 0$,

$$\int_0^\infty \big(\mathcal{B}_P[P] + \mathcal{B}_W[P]\big)(t,x)\,dx = 2\,\lambda_P\big(\bar{W}(t)\big)\,\bar{P}(t),$$

so on $\mathcal{X}_T$ or $\mathcal{X}_\infty$, the birth operators are bounded with norm controlled by λ_P.

(iii) Local existence: For any $R > 0$ and initial data (P_0, W_0) with $\|P_0\| + \|W_0\| \leq R$, there exists $T = T(R) > 0$ such that the transport system admits a unique local solution

$$(P(t,\cdot), W(t,\cdot)) \in \mathcal{X}_T, \quad \|(P,W)\|_{\mathcal{X}_T} \leq 2R.$$

Proof. (i) The nonlinearities p_i $(i = 1,2,3)$, λ_P, and λ_R on $[0,\infty)$ can be extended to globally Lipschitz functions on $\mathbb{R}$. Specifically, define the extensions:

$$\tilde{p}_i(x) := p_i(x_+), \quad \tilde{\lambda}_P(x) := \lambda_P(x_+), \quad \tilde{\lambda}_R(x) := \lambda_R(x_+),$$

where $x_+ = \max\{x, 0\}$. Since each of $p_1, p_2, \lambda_P, \lambda_R$ is C^1 and bounded on $[0,\infty)$, the following definition is introduced

$$L_1 := \sup_{x\geq 0} |p_1'(x)|, \quad L_2 := \sup_{x\geq 0} |p_2'(x)|, \quad L_3 := \sup_{x\geq 0} |\lambda_P'(x)|, \quad L_4 := \sup_{x\geq 0} |\lambda_R'(x)|.$$

Define the truncation map $T : \mathbb{R} \to [0,\infty)$ by $T(x) = x_+$. Note that T is Lipschitz with constant 1. Then the extensions $\tilde{p}_1, \tilde{p}_2, \tilde{\lambda}_P, \tilde{\lambda}_R$ are globally Lipschitz on $\mathbb{R}$ with Lipschitz constant L_1, L_2, L_3, L_4, respectively. Finally, because $p_3 = 1 - p_1 - p_2$ on $[0,\infty)$, the corresponding extension $\tilde{p}_3$ has the Lipschitz constant $L_1 + L_2$.

(ii) This follows from applying the change of variable $y = x/\alpha$ in each term of the integral and using the properties of the delta kernels.

(iii) Local existence is used in Step 5 of Theorem 1. It establishes the local existence of solutions under a mass bound on the initial data, and is proved in Step 1 of the same theorem.

□

2.2. Existence, Uniqueness, Positivity, and L^1 Bounds

The preparatory lemmas above provide the analytic foundation: the nonlinear coefficients are globally Lipschitz after extension, and the local existence of solutions. With these tools, the global theory is established.

Theorem 1 (Global well-posedness in $\mathcal{X}_\infty$)**.** *Assume* (H1)–(H2)*. Then the PDE system admits a unique global solution*

$$(P, W) \in C([0,\infty); L^1([0,\infty)) \times L^1([0,\infty))).$$

The solution remains nonnegative for all $t \geq 0$ and satisfies the a priori mass bound

$$M(t) \leq e^{2\hat{\lambda}_P t} M_0, \quad \forall\, t \geq 0$$

for $M(t) = \bar{P}(t) + \bar{W}(t)$, $M_0 = \|P_0\| + \|W_0\|$. Moreover, the total populations $\bar{P}$ and $\bar{W}$ are absolutely continuous in t and obey the following balance laws for a.e. $t \geq 0$:

$$\begin{cases} \dfrac{d\bar{P}}{dt} = \Big[p_1(\bar{W}) - p_2(\bar{W})\Big]\lambda_P(\bar{W})\bar{P} + \lambda_R(\bar{P})\bar{W}, & t > 0, \\ \dfrac{d\bar{W}}{dt} = \Big[1 - p_1(\bar{W}) + p_2(\bar{W})\Big]\lambda_P(\bar{W})\bar{P} - \lambda_R(\bar{P})\bar{W} - \displaystyle\int_0^\infty \delta(x) W(t,x)\, dx, & t > 0, \\ \bar{P}(0) = \bar{P}_0 = \|P_0\|,\ \bar{W}(0) = \bar{W}_0 = \|W_0\|. \end{cases} \tag{9}$$

Proof. The proof is organized into steps:

(i) Define the Picard map on $\mathcal{X}_T = C([0,T]; L^1 \times L^1)$ by a mild formulation along characteristics.
(ii) Use Lipschitz feedback and change-of-variable formulas in the nonlocal births to show the map is a contraction for small T.
(iii) Positivity is invariant by construction.
(iv) Pass from mild to weak formulations and derive exact balance laws for total counts.
(v) Obtain an a priori mass bound $M'(t) \leq a\, M(t)$; Grönwall ensures $\sup_{t\in[0,T]} M(t) < \infty$.
(vi) Iterate the local solution using the bound to cover all $t > 0$.

To avoid confusion in notation, we emphasize that both (P, W) and $(\bar{P}, \bar{W})$ appear in the proof. Here, $P(t,x)$ and $W(t,x)$ denote the stem and TD cell density functions over the damage variable x, while $\bar{P}(t) = \int_0^\infty P(t,x)\, dx$ and $\bar{W}(t) = \int_0^\infty W(t,x)\, dx$ represent their corresponding total population counts.

Step 1: Contraction. The proof begins by employing the Picard map Ψ, defined by the following formulas

$$\begin{aligned} P(t,x) &= \exp(-\Lambda_P[W](0;t))P_0(x - v_P t)\mathbf{1}_{x \geq v_P t} \\ &\quad + \int_0^t \exp(-\Lambda_P[W](s;t))\big(\mathcal{B}_P[P] + \lambda_R(s)W\big)(s, X_P(s;t,x))\mathbf{1}_{x \geq v_P(t-s)}\, ds, \end{aligned} \tag{10}$$

$$\begin{aligned} W(t,x) &= \exp(-\Lambda_W[P](0;t,x))W_0(x - v_W t)\mathbf{1}_{x \geq v_W t} \\ &\quad + \int_0^t \exp(-\Lambda_W[P](s;t,x))\, \mathcal{B}_W[P](s, X_W(s;t,x))\mathbf{1}_{x \geq v_W(t-s)}\, ds. \end{aligned} \tag{11}$$

along the characteristic lines

$$X_P(s;t,x) = x - v_P(t-s),$$
$$X_W(s;t,x) = x - v_W(t-s), \quad 0 \le s \le t.$$

Here, $\Lambda_P[W](s;t)$ and $\Lambda_W[P](s;t,x)$ are defined as

$$\Lambda_P[W](s;t) := \int_s^t \lambda_P(\bar{W}(\tau))\, d\tau,$$
$$\Lambda_W[P](s;t,x) := \int_s^t \left(\delta(X_W(\tau;t,x)) + \lambda_R(\bar{P}(\tau))\right) d\tau.$$

and involves the global Lipschitz extensions $\tilde{p}_i$, $\tilde{\lambda}_P$, $\tilde{\lambda}_R$ (notation simplified by dropping tildes, justified after Step 2).

To be precise, define

$$\Psi : (P,W) \in \mathcal{X}_T \mapsto (\widetilde{P},\widetilde{W}) = S_0 + F(P,W),$$

where

$$S_0(t,x) := \begin{pmatrix} \exp(-\Lambda_P[W](0;t))P_0(x - v_P t)\mathbf{1}_{x \ge v_P t} \\ \exp(-\Lambda_W[P](0;t,x))W_0(x - v_W t)\mathbf{1}_{x \ge v_W t}) \end{pmatrix},$$

and F represents the birth and reaction terms in (10) and (11) with nonlinearities evaluated at (P,W).

For two pairs $(P_j,W_j) \in \mathcal{X}_T, j = 1,2$, their images under Ψ are denoted by $(\widetilde{P}_i,\widetilde{W}_i)$. Introduce

$$p_i^j(t) := p_i(\bar{W}_j(t)), \quad p_3^j(t) = 1 - p_1^j(t) - p_2^j(t),$$
$$\lambda_P^j(t) := \lambda_P(\bar{W}_j(t)), \quad \lambda_R^j(t) := \lambda_R(\bar{P}_j(t)).$$

to ease notation. Also define

$$\Lambda_P^j(s;t) := \int_s^t \lambda_P^j(\tau)\, d\tau,$$
$$\Lambda_W^j(s;t,x) := \int_s^t \left(\delta(X_W(\tau;t,x)) + \lambda_R^j(\tau)\right) d\tau.$$

For each $j = 1,2$, corresponding to the two candidate solutions (P_j,W_j), define the nonlocal birth operators as $\mathcal{B}_P^j[P_j]$ and $\mathcal{B}_W^j[P_j]$ using the coefficients $p_i^j(t)$ and $\lambda_P^j(t)$ evaluated at $\bar{W}_j(t)$:

$$\mathcal{B}_P^j[P_j](t,x) := \frac{p_1^j(t)\lambda_P^j(t)}{\alpha_1}P_j(t,x/\alpha_1) + \frac{p_1^j(t)\lambda_P^j(t)}{\alpha_2}P_j(t,x/\alpha_2) + \frac{p_3^j(t)\lambda_P^j(t)}{\gamma_1}P_j(t,x/\gamma_1),$$

$$\mathcal{B}_W^j[P_j](t,x) := \frac{p_2^j(t)\lambda_P^j(t)}{\beta_1}P_j(t,x/\beta_1) + \frac{p_2^j(t)\lambda_P^j(t)}{\beta_2}P_j(t,x/\beta_2) + \frac{p_3^j(t)\lambda_P^j(t)}{\gamma_2}P_j(t,x/\gamma_2).$$

Write

$$F(P_1,W_1) - F(P_2,W_2) = (F_1(P_1,W_1;P_2,W_2), F_2(P_1,W_1;P_2,W_2))$$

with

$$
\begin{aligned}
&F_1(P_1, W_1; P_2, W_2)\\
&= \underbrace{\exp(-\Lambda_P^1(0;t))P_0(x - v_P t)\mathbf{1}_{x \geq v_P t} - \exp(-\Lambda_P^2(0;t))P_0(x - v_P t)\mathbf{1}_{x \geq v_P t}}_{A_1}\\
&+ \underbrace{\int_0^t \left[\exp(-\Lambda_P^1(s;t))\mathcal{B}_P^1[P_1](s, X_P(s;t,x)) - \exp(-\Lambda_P^2(s;t))\mathcal{B}_P^2[P_2](s, X_P(s;t,x))\right]\mathbf{1}_{x \geq v_P(t-s)}\, ds}_{A_2}\\
&+ \underbrace{\int_0^t \left[\exp(-\Lambda_P^1(s;t))\lambda_R^1(s)W_1(s, X_P(s;t,x)) - \exp(-\Lambda_P^2(s;t))\lambda_R^2(s)W_2(s, X_P(s;t,x))\right]\mathbf{1}_{x \geq v_P t}\, ds}_{A_3},
\end{aligned}
$$

$$
\begin{aligned}
&F_2(P_1, W_1; P_2, W_2)\\
&= \underbrace{\left[\exp(-\Lambda_W^1(0;t,x)) - \exp(-\Lambda_W^2(0;t,x))\right]W_0(x - v_W t)\mathbf{1}_{x \geq v_W t}}_{B_1}\\
&+ \underbrace{\int_0^t \left[\exp(-\Lambda_W^1(s;t,x))\mathcal{B}_W^1[P_1](s, X_W(s;t,x)) - \exp(-\Lambda_W^2(s;t,x))\mathcal{B}_W^2[P_2](s, X_W(s;t,x))\right]\mathbf{1}_{x \geq v_W(t-s)}\, ds}_{B_2}.
\end{aligned}
$$

Each A_i, B_i is next estimated in the L^1-norm, uniformly for $t \in [0, T]$. The strategy is standard: expand differences, use the mean value theorem, and apply the Lipschitz bounds from Lemma 1 and the following integral identities, such as

$$
\begin{aligned}
\int_0^\infty P_0(x - v_P t)\mathbf{1}_{x \geq v_P t}\, dx &= \|P_0\|,\\
\int_0^\infty \frac{1}{\alpha} P(s, X_P(s;t,x)/\alpha)\mathbf{1}_{x \geq v_P(t-s)}\, dx &= \|P(s,\cdot)\|,
\end{aligned}
$$

where the second identity follows from the change of variable $y = X_P(s;t,x)/\alpha_1$:

$$
\begin{aligned}
\int_0^\infty \frac{1}{\alpha} P_1(s, X_P(s;t,x)/\alpha_1)\mathbf{1}_{x \geq v_P(t-s)}\, dx &= \int_{\frac{-v_P(t-s)}{\alpha_1}}^\infty P_1(s,y)\mathbf{1}_{y \geq 0}\, dy\\
&= \int_0^\infty P_1(s,y)\, dy = \|P_1(s,\cdot)\|.
\end{aligned}
$$

First, the L^1-norm of A_1 on $[0, T]$ is estimated:

$$
\begin{aligned}
\|A_1\| &= \int_0^\infty P_0(x - v_P t)\mathbf{1}_{x \geq v_P t} |\exp(-\Lambda_P^1(0;t)) - \exp(-\Lambda_P^2(0;t))|\, dx\\
&\leq \int_0^\infty P_0(x - v_P t)\mathbf{1}_{x \geq v_P t} \int_0^t |\lambda_P^1(s) - \lambda_P^2(s)|\, ds\, dx\\
&\leq L_3 \int_0^t |\bar{P}_1(s) - \bar{P}_2(s)| \int_0^\infty P_0(x - v_P t)\mathbf{1}_{x \geq v_P t}\, dx\, ds.
\end{aligned}
$$

Taking the sup over $t \in [0, T]$ gives

$$
\sup_{t \in [0,T]} \|A_1\| \leq L_3 \|P_0\| T \sup_{t \in [0,T]} \|P_1(t,\cdot) - P_2(t,\cdot)\| \leq L_3 \|P_0\| T\, \|(P_1, W_1) - (P_2, W_2)\|_{\mathcal{X}_T}.
$$

Here, the following fact is used:

$$|\bar{P}_1(s) - \bar{P}_2(s)| \le \int_0^\infty |P_1(s,x) - P_2(s,x)|\, dx = \|P_1(s,\cdot) - P_2(s,\cdot)\|.$$

The analysis now proceeds for A_2. Decompose A_2 as

$$A_2 = \underbrace{\int_0^t \Big[\exp(-\Lambda_P^1(s;t)) - \exp(-\Lambda_P^2(s;t))\Big] \mathcal{B}_P^1[P_1](s, X_P(s;t,x)) \mathbf{1}_{x \ge v_P(t-s)}\, ds}_{A_{2,1}}$$
$$+ \underbrace{\int_0^t \exp(-\Lambda_P^2(s;t)) \Big[\mathcal{B}_P^1[P_1](s, X_P(s;t,x)) - \mathcal{B}_P^2[P_2](s, X_P(s;t,x))\Big] \mathbf{1}_{x \ge v_P(t-s)}\, ds}_{A_{2,2}}$$

The term $A_{2,1}$ admits the following decomposition:

$$A_{2,1} = \underbrace{\int_0^t \Big[\exp(-\Lambda_P^1(s;t)) - \exp(-\Lambda_P^2(s;t))\Big] \frac{p_1^1(s)\lambda_P^1(s)}{\alpha_1} P_1(s, X_P(s;t,x)/\alpha_1) \mathbf{1}_{x \ge v_P(t-s)}\, ds}_{A_{2,1,1}}$$
$$+ \underbrace{\int_0^t \Big[\exp(-\Lambda_P^1(s;t)) - \exp(-\Lambda_P^2(s;t))\Big] \frac{p_1^1(s)\lambda_P^1(s)}{\alpha_2} P_1(s, X_P(s;t,x)/\alpha_2) \mathbf{1}_{x \ge v_P(t-s)}\, ds}_{A_{2,1,2}}$$
$$+ \underbrace{\int_0^t \Big[\exp(-\Lambda_P^1(s;t)) - \exp(-\Lambda_P^2(s;t))\Big] \frac{p_3^1(s)\lambda_P^1(s)}{\gamma_1} P_1(s, X_P(s;t,x)/\gamma_1) \mathbf{1}_{x \ge v_P(t-s)}\, ds}_{A_{2,1,3}}$$

The term $A_{2,1,1}$ is estimated:

$$\begin{aligned}\|A_{2,1,1}(t,\cdot)\| &\le \int_0^t \int_0^\infty \Big|\exp(-\Lambda_P^1(s;t)) - \exp(-\Lambda_P^2(s;t))\Big| \\ &\quad \times \frac{\hat{p}_1 \hat{\lambda}_P}{\alpha_1} |P_1(s, X_P(s;t,x)/\alpha_1)| \mathbf{1}_{x \ge v_P(t-s)}\, dx\, ds \\ &\le L_3 \hat{p}_1 \hat{\lambda}_P \int_0^t \int_s^t \|W_1(\tau,\cdot) - W_2(\tau,\cdot)\|\, d\tau \cdot \|P_1(s,\cdot)\|\, ds.\end{aligned}$$

Taking the supremum over $t \in [0,T]$ gives

$$\begin{aligned}\sup_{t\in[0,T]} \|A_{2,1,1}(t,\cdot)\| &\le \hat{p}_1 \hat{\lambda}_P L_3 \|(P_1,W_1)\|_{\mathcal{X}_T} \|(P_1,W_1) - (P_2,W_2)\|_{\mathcal{X}_T} \int_0^T (T-s)\, ds \\ &\le \tfrac{1}{2}\, \hat{p}_1 \hat{\lambda}_P L_3\, T^2 \|(P_1,W_1)\|_{\mathcal{X}_T} \|(P_1,W_1) - (P_2,W_2)\|_{\mathcal{X}_T}.\end{aligned}$$

By the same argument as for $A_{2,1,1}$ (collapsing the mean-value/inner-integral steps), one obtains symmetric bounds for the other two terms. Combining these three estimates gives the compact bound

$$\sup_{t\in[0,T]} \|A_{2,1}(t,\cdot)\| \le \tfrac{1}{2}(2\hat{p}_1 + 1)\hat{\lambda}_P L_3\, T^2\, \|(P_1,W_1)\|_{\mathcal{X}_T} \|(P_1,W_1) - (P_2,W_2)\|_{\mathcal{X}_T}.$$

Similar procedures yields the bounds for $A_{2,2}$:

$$\begin{aligned}\sup_{t\in[0,T]} \|A_{2,2}(t,\cdot)\| \le \Big((3L_1 + L_2)\hat{\lambda}_P \|(P_1,W_1)\|_{\mathcal{X}_T} + (2\hat{p}_1+1)L_3\hat{p}_1 \|(P_1,W_1)\|_{\mathcal{X}_T} \\ + (2\hat{p}_1+1)\hat{\lambda}_P\Big)\, T\, \|(P_1,W_1) - (P_2,W_2)\|_{\mathcal{X}_T}.\end{aligned}$$

The sup-norm of A_2 is given by

$$\sup_{t\in[0,T]}\|A_2(t,\cdot)\| \le \Big[\tfrac{1}{2}(2\hat{p}_1+1)\hat{\lambda}_P L_3 T^2\|(P_1,W_1)\|_{\mathcal{X}_T} + T\Big((3L_1+L_2)\hat{\lambda}_P + (2\hat{p}_1+1)L_3\hat{p}_1\Big)\|(P_1,W_1)\|_{\mathcal{X}_T} + (2\hat{p}_1+1)\hat{\lambda}_P T\Big]\,\|(P_1,W_1)-(P_2,W_2)\|_{\mathcal{X}_T}.$$

Similar procedures yield the bounds for A_3, B_1, and B_2. Therefore, combining the estimate for A_i, B_i, it follows that for $(P_1,W_1),(P_2,W_2)\in\mathcal{X}_T$,

$$\|\Psi(P_1,W_1)-\Psi(P_2,W_2)\|_{\mathcal{X}_T} \le C((P_i,W_i),T)\|(P_1,W_1)-(P_2,W_2)\|_{\mathcal{X}_T}. \tag{12}$$

Let $M_0 = \|P_0\|+\|W_0\|$. On the closed ball $\overline{\mathbb{B}}(0,2M_0)\subset\mathcal{X}_T$ of radius $2M_0$, the constant C in Equation (12) can be written as $C(M_0,T)$. Choosing $T_0>0$ to be sufficiently small such that $C(M_0,T)<1$ for all $T\in[0,T_0]$, then the Picard map Ψ is a strict contraction on $\overline{\mathbb{B}}(0,2M_0)$. By the Banach fixed point theorem, there exists a unique solution on $\mathcal{X}_{T_0}$.
Step 2: Positivity. The solution is shown to remain nonnegative for all $t\in[0,T_0]$. The analysis is conducted in the ordered space

$$X = L^1([0,\infty))\times L^1([0,\infty))$$

with its natural cone $X_+ = L^1_+([0,\infty))\times L^1_+([0,\infty))$. The iteration is initiated from $(P^{(0)},W^{(0)})=(0,0)$. Assume $(P^{(n)},W^{(n)})\ge 0$. Iterate $(P^{(n+1)},W^{(n+1)})$ as

$$P^{(n+1)}(t,x) = \exp(-\Lambda_P[W^{(n)}](0;t))P_0(x-v_Pt)\mathbf{1}_{x\ge v_Pt} + \int_0^t \exp(-\Lambda_P[W^{(n)}](s;t))\big(\mathcal{B}_P[P^{(n)}]+\lambda_R(s)W^{(n)}\big)(s,X_P(s;t,x))\mathbf{1}_{x\ge v_P(t-s)}\,ds,$$

$$W^{(n+1)}(t,x) = \exp(-\Lambda_W[P^{(n)}](0;t,x))W_0(x-v_Wt)\mathbf{1}_{x\ge v_Wt} + \int_0^t \exp(-\Lambda_W[P^{(n)}](s;t,x))\,\mathcal{B}_W[P^{(n)}](s,X_W(s;t,x))\mathbf{1}_{x\ge v_W(t-s)}\,ds.$$

Since the nonlinearities p_i, λ_P, and λ_R are nonnegative, and initial data $P_0\ge 0, W_0\ge 0$, all terms on the right-hand sides in $(P^{(n+1)},W^{(n+1)}) = \Psi(P^{(n)},W^{(n)})$ are nonnegative whenever $(P^{(n)},W^{(n)})\ge 0$. This proves by induction that $(P^{(n)},W^{(n)})\ge 0$ for all n. Banach fixed point theorem implies that $\{(P^{(n)},W^{(n)})\}_n$ converges to the unique solution (P,W) in $\mathcal{X}_{T_0}$. Convergence in $\mathcal{X}_{T_0}$ means

$$P^{(n)}(t,\cdot)\to P(t,\cdot)\text{ in }L^1([0,\infty)),$$

$$W^{(n)}(t,\cdot)\to W(t,\cdot)\text{ in }L^1([0,\infty)),$$

uniformly in $t\in[0,T_0]$. Since the cone X_+ is closed in X, the limit also satisfies

$$(P,W)(t,\cdot)\in L^1_+([0,\infty))\times L^1_+([0,\infty))\quad\forall\, t\in[0,T_0].$$

Because (P,W) remains nonnegative during the iteration, the arguments $(\bar{P},\bar{W})$ of the nonlinearities p_i,λ_P,λ_R remains in $[0,\infty)$. Consequently, the extended Lipschitz versions $\tilde{p}_i,\tilde{\lambda}_P,\tilde{\lambda}_R$ introduced in Lemma 1 coincide with the original coefficients along the solution trajectory:

$$\tilde{p}_i(\bar{W}(t)) = p_i(\bar{W}(t)), \quad \tilde{\lambda}_P(\bar{W}(t)) = \lambda_P(\bar{W}(t)), \quad \tilde{\lambda}_R(\bar{P}(t)) = \lambda_R(\bar{P}(t)).$$

Therefore, the fixed point constructed in Step 1 is a genuine solution of the original PDE system, not merely of the extended one.

Step 3: Weak formulations. Repeating the same arguments in Step 1 for the Picard map defined by the following formulas

$$\begin{aligned} P(t,x) = {} & P_0(x - v_P t)\mathbf{1}_{x \geq v_P t} + \int_0^t \mathcal{B}_P[P]\big(\tau, X_P(\tau;t,x)\big)\mathbf{1}_{x \geq v_P(t-\tau)}\, d\tau \\ & + \int_0^\infty \Big\{ -\lambda_P(\tau)P\big(\tau, X_P(\tau;t,x)\big) + \lambda_R(\tau)W\big(\tau, X_P(\tau;t,x)\big)\Big\}\mathbf{1}_{x \geq v_P(t-\tau)}\, d\tau, \end{aligned} \tag{13}$$

$$\begin{aligned} W(t,x) = {} & W_0(x - v_W t)\mathbf{1}_{x \geq v_W t} + \int_0^t \mathcal{B}_W[P]\big(\tau, X_W(\tau;t,x)\big)\mathbf{1}_{x \geq v_W(t-\tau)}\, d\tau \\ & + \int_0^\infty \Big\{ -\delta(X_W(\tau;t,x))W\big(\tau, X_W(\tau;t,x)\big) - \lambda_R(\tau)W\big(\tau, X_W(\tau;t,x)\big)\Big\}\mathbf{1}_{x \geq v_W(t-\tau)}\, d\tau. \end{aligned} \tag{14}$$

also yield a unique local solution. Uniqueness implies that the local solutions given by (10) and (11) and by (13) and (14) coincide. The weak formulation is verified for the local solution by employing (13) and (14). Specifically, let $T > 0$, for $\xi \in C_c^\infty((0,T) \times (0,\infty))$, the weak formulation holds:

$$\int_0^T \int_0^\infty P(\partial_t \xi + v_P \partial_x \xi)\, dxdt + \int_0^T \int_0^\infty g_P \xi\, dxdt = 0,$$

$$\int_0^T \int_0^\infty W(\partial_t \xi + v_W \partial_x \xi)\, dxdt + \int_0^T \int_0^\infty g_W \xi\, dxdt = 0,$$

where

$$g_P(t,x) := \mathcal{B}_P[P](t,x) - \lambda_P(t)P(t,x) + \lambda_R(t)W(t,x),$$

$$g_W(t,x) := \mathcal{B}_W[P](t,x) - \delta(x)W(t,x) - \lambda_R(t)W(t,x).$$

The analysis focuses on P, and the argument for W is analogous. P is written as the sum of two parts:

$$P = P^{(0)} + P^{(g)}, \quad P^{(0)}(t,x) = P_0(x - v_P t)\mathbf{1}_{x \geq v_P t}, \quad P^{(g)}(t,x) = \int_0^t g_P(\tau, X_P(\tau;t,x))\mathbf{1}_{x \geq v_P(t-\tau)}\, d\tau.$$

For the transport part $P^{(0)}$, setting $y = x - v_P t$ yields

$$\begin{aligned} I_0 := {} & \int_0^T \int_0^\infty P^{(0)}(\partial_t \xi + v_P \partial_x \xi)\, dxdt = \int_0^\infty \int_0^T P_0(y)(\partial_t \xi + \partial_x \xi)(t, y + v_P t)\, dtdy \\ = {} & \int_0^\infty P_0(y) \int_0^T \frac{d}{dt}\xi(t, y + v_P t)\, dtdy = \int_0^\infty P_0(y)[\xi(T, y + v_P T) - \xi(0,y)]\, dy = 0 \end{aligned}$$

since ξ has compact support. Next, the source term $P^{(g)}$ is used to compute

$$\begin{aligned} I_g := {} & \int_0^T \int_0^\infty P^{(g)}(\partial_t \xi + v_P \partial_x \xi)\, dxdt \\ = {} & \int_0^\infty \int_0^T \left[\int_0^t g_P(\tau, X_P(\tau;t,x))\, d\tau\right](\partial_t \xi + v_P \partial_x \xi)\, dtdx. \end{aligned}$$

Changing variables and using Fubini's theorem:

$$\begin{aligned} I_g &= \int_0^T \int_0^\infty g_P(\tau, y) \left[\int_{t=\tau}^T \frac{d}{dt} \xi(t, y + v_P(t-\tau))\, dt \right] dy d\tau \\ &= \int_0^T \int_0^\infty g_P(\tau, y) \Big[\xi(T, y + v_P(T-\tau)) - \xi(\tau, y) \Big] dy d\tau \\ &= -\int_0^T \int_0^\infty g_P(t, x) \xi(t, x)\, dx dt. \end{aligned}$$

Thus, the weak formulation for P is obtained.

Step 4: Balance law. The functions $\bar{P}$ and $\bar{W}$ are absolutely continuous and satisfy exact balance laws.

Let ψ_R be a smooth cutoff with $0 \le \psi_R \le 1$, $\psi_R(x) \equiv 1$ for $x \in [0, R]$, $\operatorname{supp} \psi_R \in [0, R+1]$, $|\psi_R'| \le C$, where C is independent of R. Define

$$F_R(t) := \int_0^\infty P(t, x) \psi_R(x)\, dx.$$

Testing the weak formulation with $\varphi(t)\psi_R(x)$ for $\varphi \in C_c^\infty((0, \infty))$ gives

$$\int_0^T \int_0^\infty P(\varphi' \psi_R + v_P \varphi \psi_R')\, dx dt + \int_0^T \int_0^\infty (\mathcal{B}_P[P] - \lambda_P P + \lambda_R \bar{W}) \varphi \psi_R\, dx dt = 0.$$

By Fubini,

$$\begin{aligned} &-\int_0^T \varphi'(t) F_R(t)\, dt \\ &= \int_0^T \varphi(t) \underbrace{\left\{ v_P \int_0^\infty P(t, x) \psi_R'(x)\, dx + \int_0^\infty (\mathcal{B}_P[P] - \lambda_P \bar{P} + \lambda_R \bar{W})(t, x) \psi_R(x)\, dx \right\}}_{=: L(t)} dt. \end{aligned}$$

Since $(P, W) \in \mathcal{X}_T$, $L \in L^1([0, T])$. Hence, F_R is absolutely continuous on $[0, T]$ with, for a.e. t,

$$\begin{aligned} F_R'(t) &= L(t) \\ &= v_P \int_0^\infty P(t, x) \psi_R'(x)\, dx + \int_0^\infty (\mathcal{B}_P[P] - \lambda_P P + \lambda_R W)(t, x) \psi_R(x)\, dx. \end{aligned} \tag{15}$$

Integrating over $[0, t]$ yields

$$\begin{aligned} &\int_0^\infty P(t, x) \psi_R(x)\, dx - \int_0^\infty P_0(x) \psi_R(x)\, dx \\ &= \int_0^t \left\{ v_P \int_0^\infty P(\tau, x) \psi_R'(x)\, dx + \int_0^\infty (\mathcal{B}_P[P] - \lambda_P P + \lambda_R W)(\tau, x) \psi_R(x)\, dx \right\} d\tau. \end{aligned} \tag{16}$$

The limit is passed to each term. Since $0 \le \psi_R \le 1$ and $P \in L^1$, dominated convergence theorem gives

$$\begin{aligned} \lim_{R \to \infty} \int_0^\infty P(t, x) \psi_R(x)\, dx &= \int_0^\infty P(t, x)\, dx = \bar{P}(t), \\ \lim_{R \to \infty} \int_0^\infty P_0(x) \psi_R(x)\, dx &= \int_0^\infty P_0(x)\, dx = \bar{P}(0). \end{aligned}$$

Because ψ_R' is supported in the annulus $[R, R+1]$ and $\|P(\tau,\cdot)\|$ is uniformly bounded on $[0,T]$, $\int P\psi_R'\,dx \to 0$ uniformly in τ, so the first term on the right-hand side of Equation (16) vanishes as $R \to \infty$. For the source term, define

$$H_R := (\mathcal{B}_P[P] - \lambda_P P + \lambda_R W)\psi_R.$$

Pointwise, $H_R \to \mathcal{B}_P[P] - \lambda_P P + \lambda_R W$, and

$$|H_R| \le B_P[P] + \lambda_P P + \lambda_R W$$

$$\int_0^\infty (B_P[P] + \lambda_P P + \lambda_R W)(\tau,x)\,dx \le [(2p_1(\tau) + p_3(\tau) + 1)\lambda_P + \lambda_R]M(\tau),$$

with $M(\tau) = \|P(\tau,\cdot)\| + \|W(\tau,\cdot)\|$ uniformly bounded in τ. Hence dominated convergence (in x and τ) gives

$$\lim_{R\to\infty} \int_0^t \int_0^\infty H_R(\tau,x)\,dx d\tau = \int_0^t \int_0^\infty (\mathcal{B}_P[P] - \lambda_P P + \lambda_R W)(\tau,x)\,dx d\tau.$$

Collecting limits in Equation (16) gives the identity

$$\bar{P}(t) = \bar{P}(0) + \int_0^t G(\tau)\,d\tau, \quad G(\tau) := \int_0^\infty (\mathcal{B}_P[P] - \lambda_P P + \lambda_R W)(\tau,x)\,dx.$$

Since $G \in L^1(0,T)$, $\bar{P}$ is absolutely continuous with derivative $G(t)$ a.e., i.e.,

$$\frac{d}{dt}\bar{P}(t) = \int_0^\infty (\mathcal{B}_P[P] - \lambda_P P + \lambda_R W)(t,x)\,dx = (p_1(t) - p_2(t))\lambda_P(t)\bar{P}(t) + \lambda_R(t)\bar{W}(t).$$

Repeating the argument for W gives

$$\frac{d}{dt}\bar{W}(t) = (1 - p_1(t) + p_2(t))\lambda_P(t)\bar{P}(t) - \lambda_R(t)\bar{W}(t) - \int_0^\infty \delta(x)W(t,x)\,dx.$$

Adding both equations provides

$$\frac{dM}{dt} = \int_0^\infty (\mathcal{B}_P[P] + \mathcal{B}_W[P] - \lambda_P P - \delta W)\,dx \le 2\hat{\lambda}_P M,$$

so $M(t) \le \exp(2\hat{\lambda}_P t)M_0$ by Grönwall.

Step 5: Global existence. From Step 4, the local solution $(P,W) \in \mathcal{X}_{T_0}$ satisfies

$$M(T_0) = \|P(T_0,\cdot)\| + \|W(T_0,\cdot)\| \le e^{2\hat{\lambda}_P T_0}M_0 < \infty,$$

so no blow-up occurs at $t = T_0$.

By induction on n, assume that (P,W) is defined on $[0,T_n]$. The same bound implies $M(T_n) \le \exp(2\hat{\lambda}_P T_n)M_0 < \infty$, so Lemma 1 applies at $t = T_n$ with data $(P(T_n,\cdot), W(T_n,\cdot))$, delivering a unique extension to $[T_n, T_{n+1}]$ with

$$M(t) \le e^{2\hat{\lambda}_P t}M_0, \qquad t \in [T_n, T_{n+1}].$$

Iterating gives a strictly increasing sequence $\{T_n\}$ and a solution on $[0,T^*)$, $T^* = \sup_n T_n$.

If $T^* < \infty$, then for any $t_0 < T^*$, the a priori bound ensures a bounded mass at t_0. By choosing t_0 sufficiently close to T^*, Lemma 1 then yields an extension beyond T^*, a contradiction.

Hence $T^* = \infty$ and the solution is global. □

The following schematic summary in Figure 1 provides an overview of the global well-posedness proof.

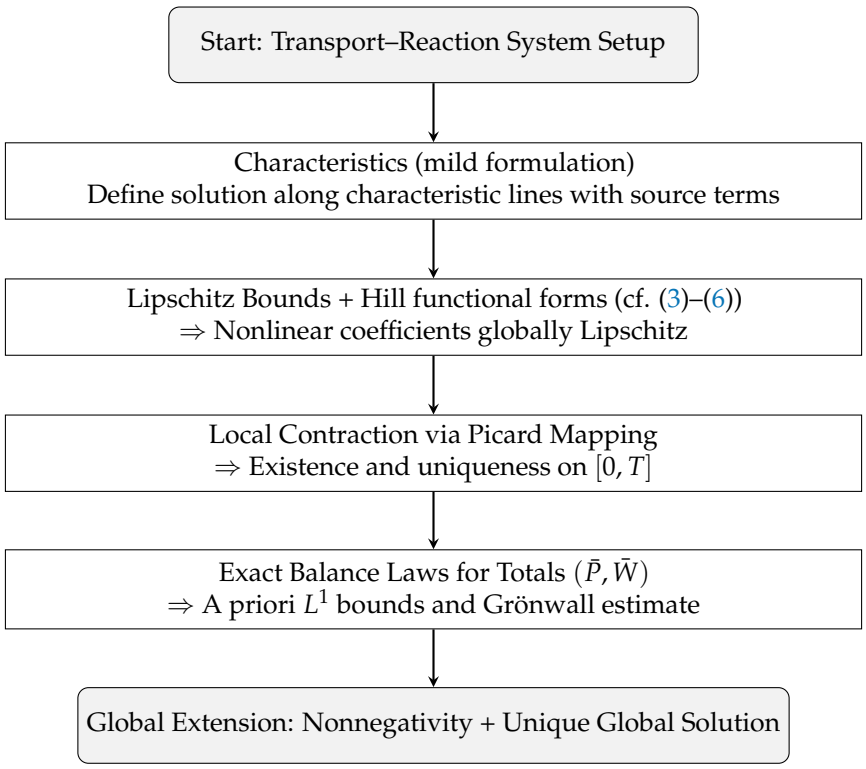


Figure 1. Method at a glance. Mild formulation → local contraction → exact balance laws → global extension.

Our global well-posedness result is established in L^1 space. Additional results in the weighted L^1 space are also included, yielding the following estimate:

Theorem 2 (Weighted L^1 estimate)**.** *Define*

$$M_1(t) := \int_0^\infty x(P(t,x) + W(t,x))\, dx.$$

Under (H1)–(H2) and assume sufficient decay for P, W, i.e., for every $t \geq 0$,

$$x(P(t,x) + W(t,x)) < \infty \quad \text{as } x \to \infty,$$

the solution (P, W) of (2) satisfies the following weighted L^1 estimate:

$$M_1(t) \leq \max\{v_P, v_W\} M(t), \quad \forall\, t \geq 0.$$

Therefore,

$$M_1(t) \leq M_1(0) + \frac{\max\{v_P, v_W\} M_0}{2\hat{\lambda}_P} \left(e^{2\hat{\lambda}_P t} - 1 \right),$$

and the weighted L^1 norm has at most exponential growth.

Proof. Multiplying the equations for P and W by x and integrating over $x \in [0, \infty)$ yields

$$\begin{aligned}
&\frac{d}{dt}\int_0^\infty xP\,dx + v_P(xP(t,x))\Big|_0^\infty - v_P\int_0^\infty P\,dx \\
&= \Big(p_1\lambda_P\alpha_1 + p_1\lambda_P\alpha_2 + p_3\lambda_P\gamma_1 - \lambda_P\Big)\int_0^\infty xP\,dx + \lambda_R\int_0^\infty xW\,dx, \\
&\frac{d}{dt}\int_0^\infty xW\,dx + v_W(xW(t,x))\Big|_0^\infty - v_W\int_0^\infty W\,dx \\
&= \Big(p_2\lambda_P\beta_1 + p_2\lambda_P\beta_2 + p_3\lambda_P\gamma_2\Big)\int_0^\infty xP\,dx - \int_0^\infty \delta(x)xW\,dx - \lambda_R\int_0^\infty xW\,dx
\end{aligned}$$

Adding the two equations yields

$$\frac{d}{dt}M_1(t) = -v_P(xP(t,x))\Big|_0^\infty - v_W(xW(t,x))\Big|_0^\infty + v_P\int_0^\infty P\,dx + v_W\int_0^\infty W\,dx - \int_0^\infty \delta(x)xW\,dx.$$

The positivity of P, W and $x(P(t,x)+W(t,x)) < \infty$ as $x \to \infty$ yields

$$\partial_t M_1(t) \le \max\{v_P, v_W\}M(t).$$

Using the L^1 norm estimate $M(t) \le e^{2\hat{\lambda}_P t}M_0$ for $t \ge 0$, the stated estimate for M_1 is easily obtained. □

Theorems 1 and 2 show that under the L^1 or weighted L^1 spaces, P and W do not become unbounded. The L^∞ estimate is a natural extension and is left for future work. The resulting balance laws in Theorem 1 for the totals $\bar{P}(t)$ and $\bar{W}(t)$ lay the foundation for the reduced system analyzed in the next section.

3. Exact Reduction to ODE

The balance laws derived from the PDE model project the dynamics of the system onto the total populations $\bar{P}$ and $\bar{W}$. However, the mortality term $\int_0^\infty \delta(x)W(t,x)\,dx$ depends on the full spatial profile of W and prevents a closed ODE in general. Under the constant death assumption $\delta(x) = \delta > 0$, however, the mortality term simplifies to $\delta\bar{W}$, allowing for an exact reduction to an autonomous two-dimensional system. The autonomous system is presented, and several results are collected (with their proof in Theorem 5):

Theorem 3 (Planar reduction and global nonoscillation under compensatory feedback)**.** *Assume $\delta(x) \equiv \delta > 0$. Then the totals $\bar{P}, \bar{W}$ obey the closed planar system*

$$\begin{cases}
\dfrac{d\bar{P}}{dt} = \Big[p_1(\bar{W}) - p_2(\bar{W})\Big]\lambda_P(\bar{W})\bar{P} + \lambda_R(\bar{P})\bar{W}, & t > 0, \\
\dfrac{d\bar{W}}{dt} = \Big[1 - p_1(\bar{W}) + p_2(\bar{W})\Big]\lambda_P(\bar{W})\bar{P} - (\lambda_R(\bar{P}) + \delta)\bar{W}, & t > 0, \\
\bar{P}(0) = \bar{P}_0 = \|P_0\|,\ \bar{W}(0) = \bar{W}_0 = \|W_0\|.
\end{cases} \tag{17}$$

obtained by integrating (1) and using $\int \delta W(t,x)\,dx = \delta\bar{W}(t)$. Suppose further that

(i) *$p_1, p_2, \lambda_P : \mathbb{R}_{\ge 0} \to \mathbb{R}_{\ge 0}$ are C^1 and nonincreasing in $\bar{W}$; $\lambda_R : \mathbb{R}_{\ge 0} \to \mathbb{R}_{\ge 0}$ is C^1 and nonincreasing in $\bar{P}$ (Hill-type laws (3)–(6) satisfy this), and $0 \le p_1 + p_2 \le 1$.*

(ii) *(Compensatory feedback) self-renewal decays more slowly than differentiation:*

$$p_1(\bar{W}) < p_2(\bar{W}), \quad \frac{dp_2(\bar{W})}{d\bar{W}} < \frac{dp_1(\bar{W})}{d\bar{W}}, \quad \forall\,\bar{W} \ge 0. \tag{18}$$

Equivalently, $p(\bar{W}) := p_1(\bar{W}) - p_2(\bar{W})$ satisfies $p(\bar{W}) < 0$ and $p'(\bar{W}) > 0$.

Then

(i) *(17) admits a unique global positive solution $(\bar{P}, \bar{W})$ that is absolutely continuous in t.*

(ii) The positive quadrant $\{\bar{P} \geq 0, \bar{W} \geq 0\}$ is forward-invariant for the flow of the system.

(iii) The system admits no nontrivial periodic orbits in $\{\bar{P} > 0, \bar{W} > 0\}$ (Dulac nonoscillation). Consequently, every bounded trajectory has an ω-limit set consisting only of equilibria and heteroclinic connections.

(iv) If, in addition, the equilibrium is unique and all solutions are bounded, the unique equilibrium is globally asymptotically stable.

Our PDE model (1) employed the constant damage accumulation speed v_P, v_W. A natural extension is the nonlinear accumulation and repair mechanism. The damage-dependent drift is decomposed into "accumulation" and "repair" components:

$$v_P(x) = a_P(x) - r_P(x), \quad v_W(x) = a_W(x) - r_W(x),$$

where $a_\cdot \geq 0$ models damage accumulation and $r_\cdot \geq 0$ models active repair. The boundary condition $v_\cdot(0) = 0$ is imposed to ensure consistency of the no-flux boundary at $x = 0$ when repair dominates at low damage. Then for any drift $v_\cdot(x)$ with $v_\cdot(0) = 0$ and sufficient decay so that the boundary flux at $x \to \infty$ vanishes, integrating (2) over x eliminates the transport term:

$$\int_0^\infty \partial_x(v_P P)\, dx = \Big[v_P P\Big]_0^\infty = 0, \quad \int_0^\infty \partial_x(v_W W)\, dx = \Big[v_W W\Big]_0^\infty = 0.$$

Consequently, the population-level ODEs for the totals remain the same as (17) under constant death rate δ. In summary, the nonlinear accumulation and repair mechanisms will impact the damage distribution in the stem and TD compartments, but yield the same total population dynamics under no-flux assumptions.

After closure, each term is interpreted in biological terms:

$$\begin{aligned} \frac{d\bar{P}}{dt} &= \underbrace{p(\bar{W})\lambda_P(\bar{W})\bar{P}}_{\text{forward self-renewal}} + \underbrace{\lambda_R(\bar{P})\bar{W}}_{\text{reverse (dedifferentiation)}}, \\ \frac{d\bar{W}}{dt} &= \underbrace{(1 - p(\bar{W}))\lambda_P(\bar{W})\bar{P}}_{\text{forward differentiation}} - \underbrace{\delta\bar{W}}_{\text{loss}} - \underbrace{\lambda_R(\bar{P})\bar{W}}_{\text{reverse sink}}. \end{aligned} \tag{19}$$

Dedifferentiation simultaneously augments $\dot{\bar{P}}$ and damps $\dot{\bar{W}}$.

This finite-dimensional reduction (17) captures self-renewal, differentiation, dedifferentiation, and constant mortality at the population level. The feedback laws in Equations (3)–(6) produce nonlinear dependence on totals while preserving exact closure. Sections 4 and 5 analyze equilibria and prove local and global stability by linearization, Dulac criterion, and the Poincaré–Bendixson theorem.

4. Local Stability and Bifurcation Threshold

With the ODE reduction in Equation (9), the linearized dynamics near equilibria are analyzed under constant δ and constant λ_R. In this section, uniform feedback on p_1, p_2 is assumed: $k_1 = k_2$ and $m_1 = m_2$. It then follows that

$$p_1(t) - p_2(t) = \frac{\hat{p}_1 - \hat{p}_2}{1 + (k_1\bar{W})^{m_1}}. \tag{20}$$

Let a nontrivial steady state $\mathcal{S} = (\bar{P}^*, \bar{W}^*)$ exist with stationary damage distributions $P^*(x)$ and $W^*(x)$. Setting $\frac{d\bar{P}}{dt} = \frac{d\bar{W}}{dt} = 0$ in Equation (17) gives

$$\begin{aligned} 0 &= \big[p_1(\bar{W}^*) - p_2(\bar{W}^*)\big]\lambda_P(\bar{W}^*)\bar{P}^* + \lambda_R\bar{W}^*, \\ 0 &= \big[1 - p_1(\bar{W}^*) + p_2(\bar{W}^*)\big]\lambda_P(\bar{W}^*)\bar{P}^* - \lambda_R\bar{W}^* - D^*, \end{aligned} \tag{21}$$

where $D^* = \int_0^\infty \delta(x)W^*(x)\,dx$. Define the W-weighted mean death rate

$$\langle\delta\rangle_{W^*} := \frac{D^*}{\bar{W}^*}. \tag{22}$$

Eliminating $\bar{P}$ from (21) yields the compact balance relation

$$(p_2(\bar{W}^*) - p_1(\bar{W}^*))\langle\delta\rangle_{W^*} = \lambda_R.$$

In the constant-death case ($\langle\delta\rangle = \delta$),

$$(p_2(\bar{W}^*) - p_1(\bar{W}^*))\delta = \lambda_R. \tag{23}$$

Here $p_1(\bar{W}^*) - p_2(\bar{W}^*) < 0$, so the left-hand side is positive. This ensures consistency with the positivity of the dedifferentiation rate $\lambda_R(\bar{P}^*) > 0$ on the right-hand side. Summing the two steady equations in (21) yields the population ratio

$$\lambda_P(\bar{W}^*)\,\bar{P}^* = D^* = \langle\delta\rangle_{W^*}\,\bar{W}^*, \qquad \Longrightarrow \qquad \frac{\bar{P}^*}{\bar{W}^*} = \frac{\langle\delta\rangle_{W^*}}{\lambda_P(\bar{W}^*)}, \tag{24}$$

so the equilibrium ratio depends only on replication and death rates at the fixed point (not on λ_R directly). Assuming feedback laws in Equations (3)–(5). The steady state is given by

$$\begin{aligned} \bar{P}^* &= \frac{\langle\delta\rangle_{W^*}\hat{W}^*}{\lambda_P(\bar{W}^*)}, \\ \bar{W}^* &= k_1^{-1}\left(\frac{(\hat{p}_2 - \hat{p}_1)\langle\delta\rangle_{W^*} - \lambda_R}{\lambda_R}\right)^{1/m_1}. \end{aligned} \tag{25}$$

The closed ODE (constant-δ reduction) is now linearized about $\mathcal{S} = (\bar{P}^*, \bar{W}^*)$. Write $p(\bar{W}) := p_1(\bar{W}) - p_2(\bar{W})$ and omit explicit $(\bar{W}^*)$ evaluation where clear. The reduced dynamics are

$$\frac{d\bar{P}}{dt} = \underbrace{p(\bar{W})\,\lambda_P(\bar{W})\,\bar{P} + \lambda_R\,\bar{W}}_{=:f_P}, \qquad \frac{d\bar{W}}{dt} = \underbrace{(1 - p(\bar{W}))\,\lambda_P(\bar{W})\,\bar{P} - (\lambda_R + \delta)\,\bar{W}}_{=:f_W}.$$

The Jacobian $\mathcal{J}(\mathcal{S})$ evaluated at $\mathcal{S}$ has entries

$$a_{11} = \partial_{\bar{P}} f_P = p\,\lambda_P, \qquad a_{12} = \partial_{\bar{W}} f_P = \bar{P}\frac{d}{d\bar{W}}(p\,\lambda_P) + \lambda_R,$$

$$a_{21} = \partial_{\bar{P}} f_W = (1 - p)\,\lambda_P, \qquad a_{22} = \partial_{\bar{W}} f_W = \bar{P}\frac{d}{d\bar{W}}((1 - p)\lambda_P) - (\lambda_R + \delta).$$

all evaluated at $(\bar{P}^*, \bar{W}^*)$. A straightforward algebraic expansion with (23) yields identities

$$\mathrm{tr}\,\mathcal{J}(\mathcal{S}) = a_{11} + a_{22} = p(\bar{W}^*)\lambda_P(\bar{W}^*) - \bar{P}^*p'(\bar{W}^*)\lambda_P(\bar{W}^*) + \bar{P}^*(1 - p(\bar{W}^*))\lambda_P'(\bar{W}) - (\lambda_R + \delta) \tag{26}$$

$$\begin{aligned} \det\mathcal{J}(\mathcal{S}) &= a_{11}a_{22} - a_{12}a_{21} = -\lambda_P(\bar{W}^*)\Big(\lambda_R + p(\bar{W}^*)\,\delta\Big) \;-\; \bar{P}^*\,\lambda_P(\bar{W}^*)^2\,p'(\bar{W}^*) \\ &= -\bar{P}^*\,\lambda_P(\bar{W}^*)^2\,p'(\bar{W}^*). \end{aligned} \tag{27}$$

Without feedback, the Jacobian at equilibrium satisfies

$$\operatorname{tr} \mathcal{J}(\mathcal{S}) = p\lambda_P - (\lambda_R + \delta) = -\frac{\lambda_P \lambda_R}{\delta} - (\lambda_R + \delta) < 0, \qquad \det \mathcal{J}(\mathcal{S}) = 0.$$

Hence, the eigenvalues are

$$\lambda_1 = 0, \qquad \lambda_2 = -\frac{\lambda_P \lambda_R}{\delta} - (\lambda_R + \delta) < 0,$$

confirming that the system has one neutral and one strictly stable direction in the non-feedback case. The zero determinant ensures that $\mathcal{J}(\mathcal{S})$ is singular; therefore, there is a continuum of equilibria, unique up to a scalar factor. With feedback, (23) yields $p(\bar{W}^*) < 0$. (20) ensures $\hat{p}_1 - \hat{p}_2 < 0$. Then, taking differentiation of p gives $p'(\bar{W}^*) > 0$, and the determinant is negative, and the equilibrium is a saddle (one unstable, one stable direction). The following result summarizes how dedifferentiation introduces a neutral direction in the absence of feedback, and how feedback then selects and reveals a saddle structure.

Theorem 4 (Local saddle revealed by feedback when dedifferentiation is present)**.** *Assume that $\delta(x) \equiv \delta > 0$ is constant. In the absence of feedback on $p_1, p_2, \lambda_P, \lambda_R$, a nontrivial equilibrium exists only when*

$$(p_2 - p_1)\,\delta = \lambda_R, \qquad \textit{i.e.} \qquad (p_1 - p_2)_{\text{crit}} = -\frac{\hat{\lambda}_R}{\delta}.$$

At this threshold, the Jacobian satisfies $\det \mathcal{J} = 0$ *and possesses one zero and one negative eigenvalue; hence, the equilibrium is non-hyperbolic and belongs to a continuous family of steady states.*

When Hill-type feedback on $p_1, p_2, \lambda_P, \lambda_R$ is introduced, this degeneracy is lifted and the equilibrium becomes a saddle point.

The above analysis establishes the local bifurcation structure: dedifferentiation creates a degenerate (non-hyperbolic) continuum of equilibria in the no-feedback limit, and feedback lifts this degeneracy and reveals a saddle. The non-hyperbolic vs, saddle structure is merely a local result under the concrete feedback on p_1, p_2, λ_P with constant λ_R and δ in this section. For the general feedback on $p_1, p_2, \lambda_P, \lambda_R$, some additional assumptions could yield globally asymptotic stability, in contrast to the local and unstable saddle classification.

If the death rate increases with damage, $\delta'(x) > 0$, highly damaged cells are removed more efficiently, shifting the stationary damage distribution toward lower x. This reduces the mean death rate $\langle \delta \rangle_{W^*}$, hence $\bar{W}^*$ decreases by (25). Since λ_P is a decreasing function of $\bar{W}$, an increasing δ function renders the decline of the stem population $\bar{P}^*$ and ratio $\bar{P}^*/\bar{W}^*$ by (24). Biologically, an increasing $\delta(x)$ promotes a lineage biased toward more differentiated cells and a more fragile stem-cell pool, consistent with age-related decline in regenerative capacity.

The global behavior of the reduced system is next considered to determine whether these local stability properties extend to the entire positive quadrant.

5. Global Stability Analysis

Extending the local results, the global dynamics of the reduced system (9) are classified under the constant death rate $\delta(x) \equiv \delta > 0$. The positive quadrant is forward-invariant because the PDE solutions remain nonnegative (Theorem 1). It is assumed that the feedback

maps $p_1, p_2, \lambda_P, \lambda_R$ are continuous, monotone decreasing, and vanish at infinity: for all $\bar{P}, \bar{W} \geq 0$,

$$p_1'(\bar{W}) < 0, \quad p_2'(\bar{W}) < 0, \quad \lambda_P'(\bar{W}) < 0, \quad \lambda_R'(\bar{P}) < 0,$$
$$\lim_{\bar{W}\to\infty} p_1(\bar{W}) = 0, \quad \lim_{\bar{W}\to\infty} p_2(\bar{W}) = 0, \quad \lim_{\bar{W}\to\infty} \lambda_P(\bar{W}) = 0, \quad \lim_{\bar{P}\to\infty} \lambda_R(\bar{P}) = 0.$$

The compensatory feedback condition (18) is imposed. Biologically, the compensatory feedback condition (18) expresses a stabilizing regulatory mechanism that maintains homeostasis in the lineage. The inequalities $p_1(\bar{W}) < p_2(\bar{W})$ and $p_1'(\bar{W}) > p_2'(\bar{W})$ together mean that as the total TD population $\bar{W}$ increases, the system responds by reducing the differentiation bias and relatively sustaining self-renewal. In other words, differentiation weakens more rapidly than self-renewal under strong feedback, providing a compensatory effect that prevents excessive depletion of stem cells when $\bar{W}$ is large.

The global asymptotic behavior under compensatory feedback is now presented. For notational clarity, the shorthand already used in Section 4 is introduced:

$$p(\bar{W}) := p_1(\bar{W}) - p_2(\bar{W}),$$

which measures the net self-renewal bias. Negative p corresponds to dominance of difference, while positive p indicates dominance of self-renewal. This notation simplifies the divergence computation and subsequent algebraic expressions.

Theorem 5 (Global asymptotic behavior under compensatory feedback)**.** *Assume the ODE reduction (Equation* (17)*) holds, with constant δ. Assume the compensatory feedback condition* (18)*. Moreover, the system admits only finite number of equilibria. Then the ω-limit set of any bounded solution $\Phi(t) = (\bar{P}(t), \bar{W}(t))$ is either a single equilibrium point, or a finite set of equilibria $\{\mathbf{q}_1, \ldots, \mathbf{q}_m\}$ connected by heteroclinic orbits.*

If, in addition, the equilibrium $\mathcal{S} = (\bar{P}^*, \bar{W}^*)$ is unique, the following dichotomy holds:

(i) Convergence: *If $\Phi(t)$ is bounded, then $\Phi(t) \to \mathcal{S}$ as $t \to \infty$, and*

$$\lim_{t\to\infty} \Big((p_2(\bar{W}(t)) - p_1(\bar{W}(t)))\delta - \lambda_R(\bar{P}(t)) \Big)$$
$$= \lim_{t\to\infty} \Big(- p(\bar{W}(t))\delta - \lambda_R(\bar{P}(t)) \Big) = 0$$

If, moreover, every solution of (9) *is bounded, then $\mathcal{S}$ is globally asymptotically stable.*

(ii) Divergence: *Conversely, if the balance relation fails asymptotically, then $\Phi(t)$ cannot remain bounded. More precisely, $\limsup_{t\to\infty} \|\Phi(t)\| \to \infty$ as $t \to \infty$, if*

$$\limsup_{t\to\infty} \big| - p(\bar{W}(t))\delta - \lambda_R(\bar{P}(t)) \big| > 0.$$

Proof. Step 1: Negative divergence and Dulac.

Let

$$\mathbf{G}(\bar{P}, \bar{W}) = (G_1, G_2),$$

with

$$G_1 = p(\bar{W})\lambda_P(\bar{W})\bar{P} + \lambda_R(\bar{P})\bar{W}, \quad G_2 = (1 - p(\bar{W}))\lambda_P(\bar{W})\bar{P} - (\delta + \lambda_R(\bar{P}))\bar{W}.$$

Then,

$$\nabla \cdot \mathbf{G} = \frac{\partial G_1}{\partial \bar{P}} + \frac{\partial G_2}{\partial \bar{W}}.$$

A straightforward calculation gives

$$\nabla \cdot \mathbf{G} = p(\bar{W})\lambda_P(\bar{W}) + \lambda_R'(\bar{P})\bar{W} - p'(\bar{W})\lambda_P(\bar{W})\bar{P} + (1 - p(\bar{W}))\lambda_P'(\bar{W})\bar{P} - (\delta + \lambda_R(\bar{P})).$$

Under compensatory feedback, $\nabla \cdot \mathbf{G} < 0$ on Ω. Hence, Dulac's criterion precludes periodic orbits.

Step 2: No homoclinic orbits. Assume Γ is a homoclinic orbit with limit point $\mathbf{q}$, and E is the interior of $\Gamma \cup \{\mathbf{q}\}$. Green's theorem yields

$$\iint_E \nabla \cdot \mathbf{G}\, d\bar{P}\, d\bar{W} = \oint_{\Gamma \cup \{\mathbf{q}\}} (G_1\, d\bar{W} - G_2\, d\bar{P}) = \int_{-\infty}^{\infty} (G_1 G_2 - G_2 G_1)\, dt = 0.$$

This contradicts $\nabla \cdot \mathbf{G} < 0$.

Step 3: Classification of ω-limit sets. With periodic and homoclinic orbits ruled out and only finitely many equilibria assumed, the Poincaré–Bendixson theorem implies that the ω-limit set of any bounded trajectory is either a single equilibrium or a finite set of equilibria connected by a countable family of heteroclinic orbits, as stated.

Step 4: Uniqueness $\Rightarrow$ convergence of bounded trajectories. If the equilibrium $\mathcal{S} = (\bar{P}^*, \bar{W}^*)$ is unique, any bounded trajectory's ω-limit set lies in $\{\mathcal{S}\}$. Hence, $\Phi(t) \to \mathcal{S}$. At equilibria

$$-p(\bar{W}(t))\delta - \lambda_R(\bar{P}(t)) = 0.$$

Continuity of p_1, p_2, λ_R along $\Phi(t)$ thus gives

$$\lim_{t \to \infty} \Big(-p(\bar{W}(t))\delta - \lambda_R(\bar{P}(t)) \Big) = 0.$$

If, moreover, every trajectory is bounded, then all trajectories converge to $\mathcal{S}$, i.e., $\mathcal{S}$ is globally asymptotically stable. The divergence result follows easily. □

For standard references, see [44] for Dulac's criterion and the (generalized) Poincaré–Bendixson theorem and [45] for monotone dynamical systems.

Theorem 6 (Global stability under uniqueness)**.** *Assume $\delta > 0$, compensatory feedback, and that at least one of $(p_1 - p_2)(\bar{W})$ and $\lambda_R(\bar{P})$ depends nontrivially on its argument. Then G_1 and G_2 share no nontrivial common factor [44], and the equilibrium $\mathcal{S}$ is unique. Then the ω–limit set of any bounded trajectory $\Phi(t) = (\bar{P}(t), \bar{W}(t))$ in the positive quadrant reduces to $\mathcal{S}$. In particular, if all solutions are bounded, $\mathcal{S}$ is globally asymptotically stable.*

Proof. For the concrete vector field

$$G_1 = p\lambda_P\bar{P} + \lambda_R\bar{W}, \quad G_2 = (1 - p)\lambda_P\bar{P} - (\delta + \lambda_R)\bar{W},$$

a necessary condition for G_1 and G_2 to have a nontrivial common factor is that the determinant of their coefficient matrix A vanishes identically. A direct computation shows that $\det A \equiv 0$ is equivalent to

$$-p(\bar{W})\delta = \lambda_R(\bar{P}), \quad \forall\, (\bar{P}, \bar{W}) \in \Omega.$$

If at least one side depends nontrivially on its argument, the equality cannot hold for all $(\bar{P}, \bar{W})$.

The following relations hold at any equilibrium $\mathcal{S} = (\bar{P}^*, \bar{W}^*)$:

$$-p(\bar{W}^*)\delta = \lambda_R(\bar{P}^*), \tag{28}$$

$$\frac{\bar{P}^*}{\bar{W}^*} = \frac{\delta}{\lambda_P(\bar{W}^*)}, \tag{29}$$

Then

(1) If both p and λ_R vary with their arguments, then (28) holds for only one pair $(\bar{P}^*, \bar{W}^*)$.
(2) If only p is non-constant, (28) fixes a unique $\bar{W}^*$, and $\bar{P}^*/\bar{W}^* = \delta/\lambda_P(\bar{W}^*)$ gives a unique $\bar{P}^*$.
(3) If only λ_R is non-constant, (28) fixes a unique $\bar{P}^*$, and the ratio law $\bar{P}^*\lambda_P(\bar{W}^*) = \delta\bar{W}^*$—whose left-hand side decreases and right-hand side increases in $\bar{W}$—yields a unique $\bar{W}^*$.

Therefore, the equilibrium is unique. Dulac's criterion and the generalized Poincaré-Bendixson theorem apply. □

A scaling invariance result for steady states under uniform rescaling of feedback strengths is now quantified.

Proposition 1 (Scaling law of the steady state)**.** *Assume the Hill type laws* (3)–(6)*. Fix all parameters except* k_1, k_2, k_3, k_4*. If* k_i *are rescaled by a common factor* $A > 0$*, then the rescaled system admits the steady state* $(\bar{P}^*/A, \bar{W}^*/A)$*.*

Proof. The rescaling gives $p_j'(\bar{W}/A) = p_j(\bar{W})$ $(j = 1, 2)$, $\lambda_P'(\bar{W}/A) = \lambda_P(\bar{W})$, $\lambda_R'(\bar{P}/A) = \lambda_R(\bar{P})$. Substituting $(\bar{P}', \bar{W}') = (\bar{P}^*/A, \bar{W}^*/A)$ into Equation (21) recovers the steady-state relations (up to a factor of $1/A$), so $(\bar{P}', \bar{W}')$ is again an equilibrium. Assuming Hill-type laws ensures p and λ_R depend nontrivially on their arguments, and Theorem 6 guarantees the uniqueness of the equilibrium. Then this uniqueness implies that the scaling of k_i inversely shifts the steady state. □

Proposition 1 provides a practical control strategy: first adjust the ratio $\frac{\bar{W}^*}{\bar{P}^*}$ by tuning $\frac{\lambda_P}{\delta}$, then the absolute sizes $(\bar{P}^*, \bar{W}^*)$ by rescaling all k_i.

The mathematical operation of rescaling feedback strength in our reduced model has concrete biological counterparts. In tissues, the effective strength of a feedback loop can be modulated by changing the abundance or availability of receptors at the niche interface. For example, receptor degradation directly attenuate niche signaling: as shown in a Drosophila germline niche, "the Tkv receptor is internalized into hub cells from the MT-nanotube surface and subsequently degraded in the hub cell lysosomes", and perturbation of this process "resulted in an overabundance of Tkv protein in GSCs and hyperactivation of a downstream signal, suggesting that the MT-nanotubes also serve a second purpose to dampen the niche signaling" [46].

The local and global stability guarantees lend themselves to empirical verification through targeted simulations.

6. Numerical Results

This section corroborates the analytical results with simulations of the reduced ODE under a constant death rate. Consider

$$\begin{cases} \dfrac{d\bar{P}(t)}{dt} = (2f(t)-1)\hat{\lambda}_P\bar{P}(t) + \hat{\lambda}_R\bar{W}(t), & t > 0, \\ \dfrac{d\bar{W}(t)}{dt} = (2-2f(t))\hat{\lambda}_P\bar{P}(t) - (\hat{\lambda}_R + \delta)\bar{W}(t), & t > 0, \\ \bar{P}(0) = \bar{P}_0,\ \bar{W}(0) = \bar{W}_0, \end{cases} \tag{30}$$

which coincides with Equation (17) since $2f(t) - 1 = p_1(t) - p_2(t) = \dfrac{2\hat{f} - 1}{1 + (k_1 \bar{W})^{m_1}}$ (Equation (7)). The simulations confirm the bifurcation threshold $\tilde{f} = 0.25$ implied by $(1 - 2\hat{f})\delta = \hat{\lambda}_R$ and reproduces the predicted scaling behavior.

To ensure consistency between the PDE and its finite-dimensional reduction, the full damage-structured PDE system is first solved, and the computed solution is then integrated over the damage variable to obtain the corresponding total-population trajectories in the ODE reduction. The damage domain $x \in [0, \tilde{A}]$ is discretized uniformly as $x_i = i\,\Delta x$ for $i = 0, 1, \ldots, N$, and the transport terms are approximated using conservative upwind finite-volume fluxes to preserve nonnegativity and total mass. Temporal evolution is advanced using an explicit scheme subject to a Courant–Friedrichs–Lewy (CFL) condition,

$$\Delta t \leq C \frac{\Delta x}{\max\{v_P, v_W\}}, \qquad 0 < C < 1.$$

The total populations at discrete times $t^n = n\Delta t$ are evaluated by numerical quadrature,

$$\bar{P}^n = \sum_{i=1}^{N} P_i^n \Delta x, \qquad \bar{W}^n = \sum_{i=1}^{N} W_i^n \Delta x, \qquad P_i^n \approx P(t^n, x_i), \quad W_i^n \approx W(t^n, x_i).$$

For phase portraits of the reduced ODE system, the governing equations are directly integrated using the adaptive Runge–Kutta method implemented in ode45 (MATLAB R2025b). All simulations are verified to respect the CFL condition, ensuring numerical stability.

Figure 2 illustrates three regimes as $\hat{f}$ crosses the analytical threshold $\tilde{f}$. For $\hat{f} > \tilde{f}$, both populations grow exponentially. For $\hat{f} = \tilde{f}$, trajectories approach a steady state. For $\hat{f} < \tilde{f}$, both populations decay to extinction. Figure 3 shows the threshold condition $(1 - 2\hat{f})\delta = \hat{\lambda}_R$ in the $(\hat{\lambda}_R, \hat{f})$ plane for several δ, which separates growth, steady state, and extinction. Figure 4 presents phase portraits with nullclines, the saddle equilibrium, and its stable and unstable manifolds, in agreement with the local analysis. Figure 5 verifies the scaling law under Hill feedback and shows that uniform rescaling of feedback strengths rescales the steady state while preserving the population ratio.

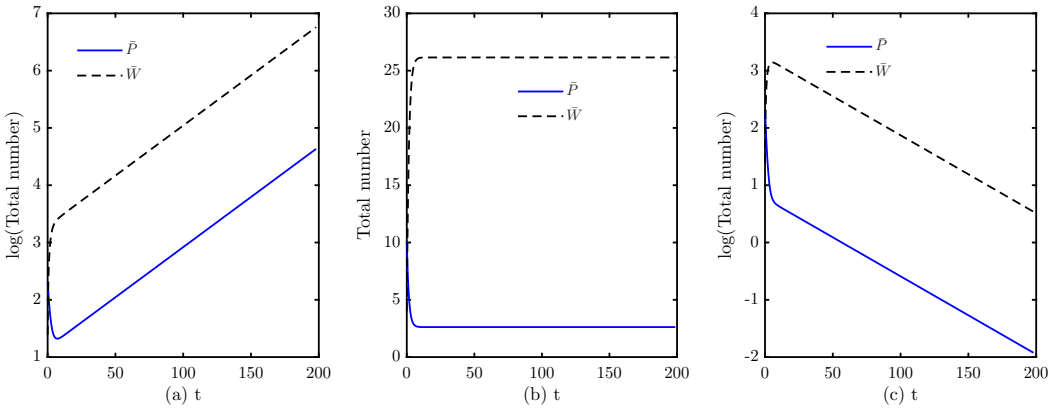


Figure 2. Bifurcation dynamics in the stem and terminally differentiated (TD) system as $\hat{f}$ crosses the threshold $\tilde{f} = 0.25$ with $\hat{\lambda}_P = 1$, $\hat{\lambda}_R = 0.05$, $\delta = 0.1$, and $\bar{P}(0) = \bar{W}(0) = 4$. (**a**) $\hat{f} > \tilde{f}$ and both populations grow exponentially, (**b**) $\hat{f} = \tilde{f}$ and the system stabilizes to a steady state, (**c**) $\hat{f} < \tilde{f}$ and populations decay exponentially towards extinction. Numerical fits confirm exponential growth or decay. A step size of $\Delta t = 0.025$ and $\Delta x = 0.01$ is used, with domain boundary $\tilde{A} = 4$. Other parameter values are $\hat{p}_1 = \tilde{f}$, $\hat{p}_2 = 1 - \tilde{f}$, $p_3 = 0$, $v_P = v_W = 0.05$, $\alpha_1 = \alpha_2 = 0.5$, $\beta_1 = \beta_2 = 0.5$, $\gamma_1 = 1/3$, $\gamma_2 = 2/3$, $k_1 = k_2 = k_3 = k_4 = 0$, $m_1 = m_2 = m_3 = m_4 = 2$.

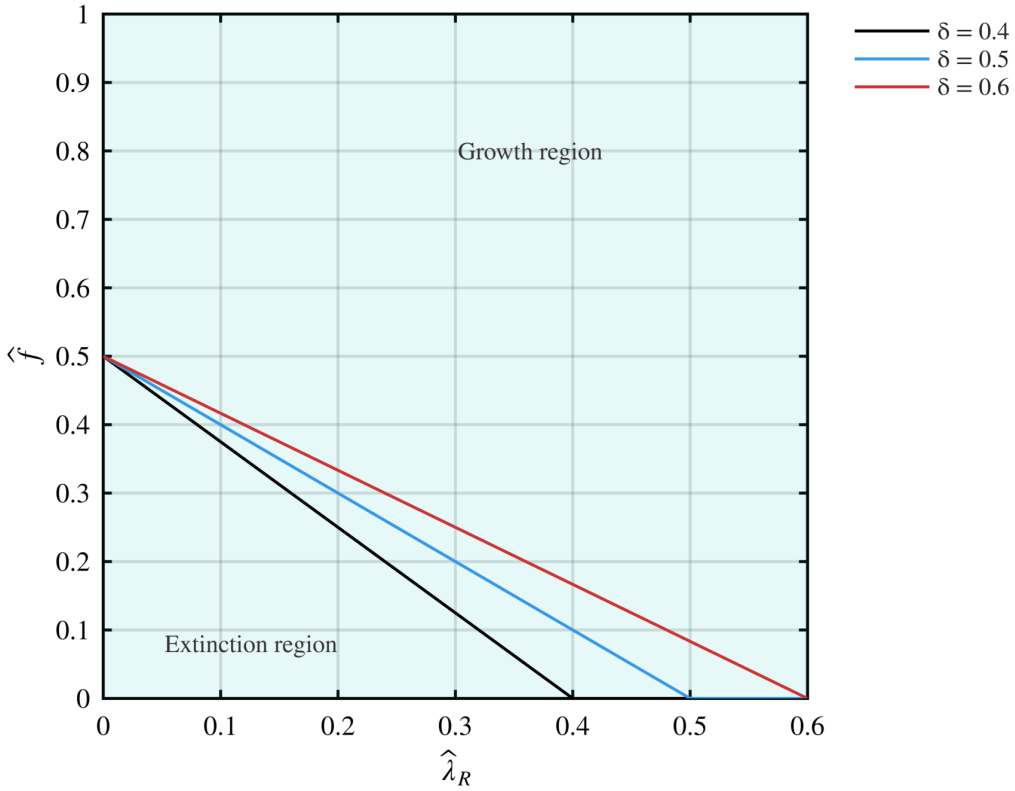


Figure 3. Bifurcation diagram in the $(\hat{\lambda}_R, \hat{f})$ plane for $\delta = 0.4$ (black), $\delta = 0.5$ (blue), and $\delta = 0.6$ (red). The curve $(1 - 2\hat{f})\delta = \hat{\lambda}_R$ separates exponential growth (above), extinction (below), and marginal equilibrium (on the line). The diagram quantifies how $\hat{f}$ and $\hat{\lambda}_R$ control transitions among three regimes.

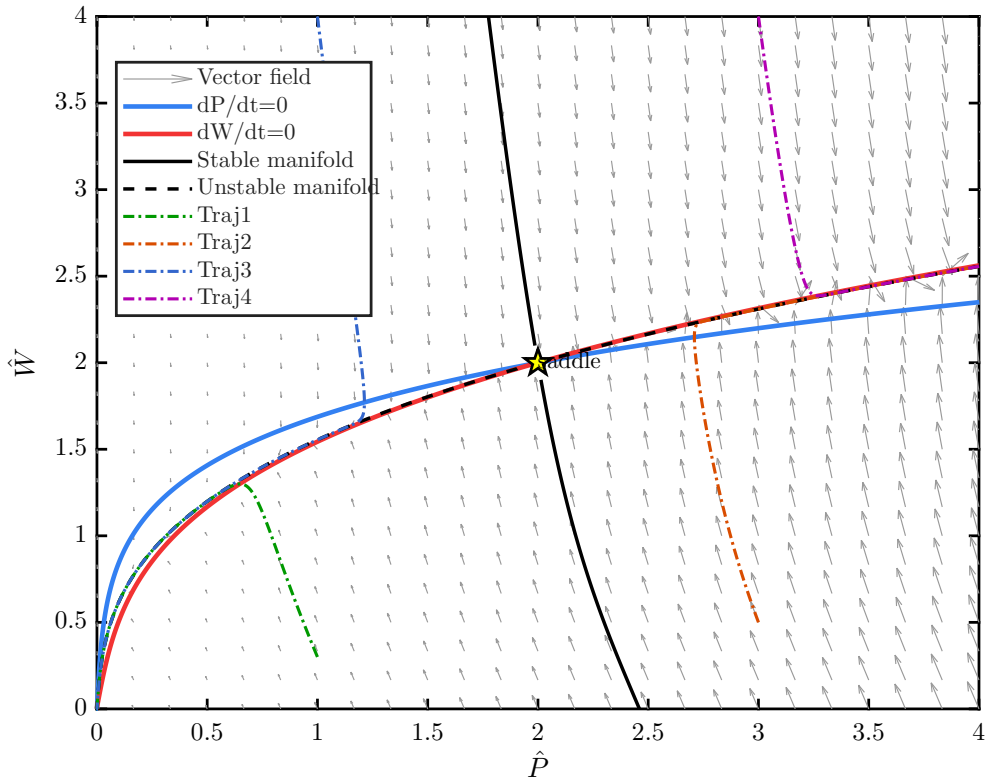


Figure 4. Phase portrait with nullclines, saddle equilibrium, and manifolds. The vector field appears in grey. The blue nullcline solves $d\bar{P}/dt = 0$ and the red nullcline solves $d\bar{W}/dt = 0$. Their intersection

marks the saddle equilibrium. The stable manifold (solid black line) forms the separatrix between bounded and unbounded trajectories, and the unstable manifold (dashed black line) repels trajectories from the equilibrium. Representative trajectories are shown as dashed colored lines. Parameters: $\hat{\lambda}_P = 1$, $\hat{\lambda}_R = 0.02$, $\delta = 0.2$, $\hat{f} = 0.25$, $\hat{p}_1 = 0.25$, $\hat{p}_2 = 0.75$, $p_3 = 0$, $k_1 = k_2 = k_3 = 1$, $k_4 = 0$, $m_1 = m_2 = m_3 = m_4 = 2$. The initial values for the four trajectories are $(\bar{P}_0, \bar{W}_0) = (1, 0.3)$ for $i = 1$, $(3, 0.5)$ for $i = 2$, $(1, 4)$ for $i = 3$, and $(3, 4)$ for $i = 4$. The Runge-Kutta method, implemented via the `ode45` solver in Matlab, is used to solve (30), so parameters v_P, v_W, α_i, β_i, γ_i are not involved. The equilibrium $(\bar{P}^*, \bar{W}^*) = (2, 2)$ satisfies $(1 - 2f(\bar{P}^*))\delta = \lambda_R(\bar{W}^*)$.

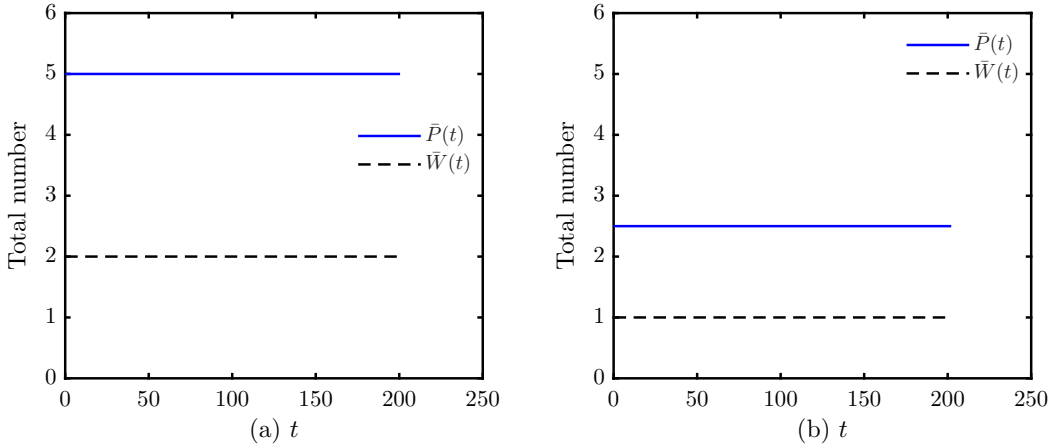


Figure 5. Numerical validation of the scaling law for Hill feedback. Trajectories of $\bar{P}(t)$ (solid) and $\bar{W}(t)$ (dashed) are shown. Rescaling the feedback parameters by a factor A rescales the steady state by $1/A$ while preserving $\bar{P}^*/\bar{W}^* = \delta/\lambda_P(\bar{W}^*)$. (**a**) For $A = 1$ with $k_1 = k_2 = k_3 = 1$, the system converges to $\mathcal{S} = (5, 2)$; (**b**) for $A = 2$ with $k_1 = k_2 = k_3 = 2$, the system converges to $\mathcal{S}' = (2.5, 1) = \mathcal{S}/2$. Parameters: $(\hat{\lambda}_P, \hat{\lambda}_R, \hat{\delta}, \hat{f}, \hat{p}_1, \hat{p}_2, p_3, v_P, v_W, \alpha_1, \alpha_2, \beta_1, \beta_2, \gamma_1, \gamma_2, m_1, m_2, m_3, m_4, \Delta t, \Delta x, \tilde{A}) = (0.4, 0.02, 0.2, 0.25, 0.25, 0.75, 0, 0.05, 0.05, 0.5, 0.5, 0.5, 0.5, 1/3, 2/3, 2, 2, 2, 2, 0.025, 0.005, 2)$.

The computations align with the theory. The algebraic threshold $(1 - 2\hat{f})\delta = \hat{\lambda}_R$ organizes the regimes, the phase portrait matches the local classification, and the uniform rescaling of feedback strengths produces the predicted steady state scaling without altering the steady population ratio. These illustrations underscore the model's predictive power, as synthesized in the conclusion.

7. Conclusions

A damage-structured transport–reaction model is introduced, coupling stem (P) and differentiated (W) cells with reversible dedifferentiation, nonlocal birth operators (damage partitioning at division), and Hill-type feedback. Main results: (i) global well-posedness in $C([0, \infty); L^1 \times L^1)$ (existence, uniqueness, positivity and an a priori mass bound); (ii) exact reduction to a two-dimensional autonomous ODE when mortality is constant, via explicit balance laws; (iii) characterization of equilibria and a bifurcation threshold separating extinction, homeostasis, and unbounded growth; (iv) global nonoscillation and, under compensatory feedback, global asymptotic stability (Dulac's criterion + Poincaré–Bendixson). Key innovations: inclusion of reversible dedifferentiation between compartments, nonlocal damage redistribution at division, and a novel steady-state scaling invariance under uniform rescaling of feedback strengths. Limitations and outlook: the ODE closure requires constant death rates; extensions to damage-dependent mortality, stochastic partitioning, variable transport speeds, demographic noise [47], or hybrid PDE–agent-based models [48] are natural next steps.

Short, testable analytical criteria and the reduction to a tractable ODE make the framework directly applicable to simulations and experimental validation.

Author Contributions: These three authors contributed equally to this work as co-first authors. Conceptualization, L.S.W. and Z.L.; methodology, J.Y. and Y.L.; software, L.S.W. and J.Y.; validation, L.S.W. and Y.L.; formal analysis, L.S.W. and J.Y.; investigation, L.S.W. and J.Y.; resources, L.S.W. and J.Y.; data curation, L.S.W. and J.Y.; writing—original draft preparation, L.S.W. and J.Y.; writing—review and editing, L.S.W. and J.Y.; visualization, L.S.W. and Y.L.; project administration, Z.L. All authors have read and agreed to the published version of the manuscript.

Funding: The research of Zonghao Liu is funded by the Major Scientific Research Program for Young and Middle-aged Health Professionals of Fujian Province, China (Grant No. 2021ZQNZD009).

Data Availability Statement: The original contributions presented in this study are included in the article. They are available under the CC-BY 4.0 license. Further inquiries can be directed to the corresponding authors.

Acknowledgments: This article was written while Jiguang Yu was visiting the STOR-i Center for Doctoral Training at Lancaster University, United Kingdom; it is a pleasure for him to thank this institution for its kind hospitality.

Conflicts of Interest: The authors declare no conflicts of interest.

Abbreviations

The following abbreviations are used in this manuscript:

CFL	Courant–Friedrichs–Lewy
ODE	Ordinary differential equation
PDE	Partial differential equation
TD	Terminally differentiated

References

1. Siebert, S.; Farrell, J.A.; Cazet, J.F.; Abeykoon, Y.; Primack, A.S.; Schnitzler, C.E.; Juliano, C.E. Stem cell differentiation trajectories in *Hydra* Resolv. Single-Cell Resolut. *Science* **2019**, *365*, eaav9314. [CrossRef]
2. Bai, Y.; Boath, J.; White, G.R.; Kariyawasam, U.G.I.U.; Farah, C.S.; Darido, C. The Balance between Differentiation and Terminal Differentiation Maintains Oral Epithelial Homeostasis. *Cancers* **2021**, *13*, 5123. [CrossRef]
3. Ashcroft, P.; Bonhoeffer, S. Constrained optimization of divisional load in hierarchically organized tissues during homeostasis. *J. R. Soc. Interface* **2022**, *19*, 20210784. [CrossRef] [PubMed]
4. Halim, A.; Ariyanti, A.D.; Luo, Q.; Song, G. Recent Progress in Engineering Mesenchymal Stem Cell Differentiation. *Stem Cell Rev. Rep.* **2020**, *16*, 661–674. [CrossRef] [PubMed]
5. Cheng, H.; Zheng, Z.; Cheng, T. New paradigms on hematopoietic stem cell differentiation. *Protein Cell* **2020**, *11*, 34–44. [CrossRef] [PubMed]
6. Lander, A.D.; Gokoffski, K.K.; Wan, F.Y.M.; Nie, Q.; Calof, A.L. Cell Lineages and the Logic of Proliferative Control. *PLoS Biol.* **2009**, *7*, e1000015. [CrossRef]
7. Dray, N.; Mancini, L.; Binshtok, U.; Cheysson, F.; Supatto, W.; Mahou, P.; Bedu, S.; Ortica, S.; Than-Trong, E.; Krecsmarik, M.; et al. Dynamic spatiotemporal coordination of neural stem cell fate decisions occurs through local feedback in the adult vertebrate brain. *Cell Stem Cell* **2021**, *28*, 1457–1472.e12. [CrossRef]
8. Navarro, T.; Iannini, A.; Neto, M.; Campoy-Lopez, A.; Muñoz-García, J.; Pereira, P.S.; Ares, S.; Casares, F. Feedback control of organ size precision is mediated by BMP2-regulated apoptosis in the Drosophila eye. *PLoS Biol.* **2024**, *22*, e3002450. [CrossRef]
9. Hannezo, E.; Heisenberg, C.P. Mechanochemical Feedback Loops in Development and Disease. *Cell* **2019**, *178*, 12–25. [CrossRef]
10. Jopling, C.; Boue, S.; Belmonte, J.C.I. Dedifferentiation, transdifferentiation and reprogramming: Three routes to regeneration. *Nat. Rev. Mol. Cell Biol.* **2011**, *12*, 79–89. [CrossRef]
11. Murata, K.; Jadhav, U.; Madha, S.; Van Es, J.; Dean, J.; Cavazza, A.; Wucherpfennig, K.; Michor, F.; Clevers, H.; Shivdasani, R.A. Ascl2-Dependent Cell Dedifferentiation Drives Regeneration of Ablated Intestinal Stem Cells. *Cell Stem Cell* **2020**, *26*, 377–390.e6. [CrossRef] [PubMed]
12. Tata, P.R.; Mou, H.; Pardo-Saganta, A.; Zhao, R.; Prabhu, M.; Law, B.M.; Vinarsky, V.; Cho, J.L.; Breton, S.; Sahay, A.; et al. Dedifferentiation of committed epithelial cells into stem cells in vivo. *Nature* **2013**, *503*, 218–223. [CrossRef] [PubMed]
13. Bensellam, M.; Jonas, J.C.; Laybutt, D.R. Mechanisms of β-cell dedifferentiation in diabetes: Recent findings and future research directions. *J. Endocrinol.* **2018**, *236*, R109–R143. [CrossRef] [PubMed]

14. Nordmann, T.M.; Dror, E.; Schulze, F.; Traub, S.; Berishvili, E.; Barbieux, C.; Böni-Schnetzler, M.; Donath, M.Y. The Role of Inflammation in β-cell Dedifferentiation. *Sci. Rep.* **2017**, *7*, 6285. [CrossRef]
15. Haddadin, L.; Sun, X. Stem Cells in Cancer: From Mechanisms to Therapeutic Strategies. *Cells* **2025**, *14*, 538. [CrossRef]
16. Malta, T.M.; Sokolov, A.; Gentles, A.J.; Burzykowski, T.; Poisson, L.; Weinstein, J.N.; Kamińska, B.; Huelsken, J.; Omberg, L.; Gevaert, O.; et al. Machine Learning Identifies Stemness Features Associated with Oncogenic Dedifferentiation. *Cell* **2018**, *173*, 338–354.e15. [CrossRef]
17. Shibue, T.; Weinberg, R.A. EMT, CSCs, and drug resistance: The mechanistic link and clinical implications. *Nat. Rev. Clin. Oncol.* **2017**, *14*, 611–629. [CrossRef]
18. Masciale, V.; Banchelli, F.; Grisendi, G.; Samarelli, A.V.; Raineri, G.; Rossi, T.; Zanoni, M.; Cortesi, M.; Bandini, S.; Ulivi, P.; et al. The molecular features of lung cancer stem cells in dedifferentiation process-driven epigenetic alterations. *J. Biol. Chem.* **2024**, *300*, 107994. [CrossRef]
19. Li, J.; Stanger, B.Z. How Tumor Cell Dedifferentiation Drives Immune Evasion and Resistance to Immunotherapy. *Cancer Res.* **2020**, *80*, 4037–4041. [CrossRef]
20. Mi, L.; Hu, J.; Li, N.; Gao, J.; Huo, R.; Peng, X.; Zhang, N.; Liu, Y.; Zhao, H.; Liu, R.; et al. The Mechanism of Stem Cell Aging. *Stem Cell Rev. Rep.* **2022**, *18*, 1281–1293. [CrossRef]
21. McNeely, T.; Leone, M.; Yanai, H.; Beerman, I. DNA damage in aging, the stem cell perspective. *Hum. Genet.* **2020**, *139*, 309–331. [CrossRef]
22. Chatterjee, B.; Thakur, S.S. Aging of hematopoietic stem cells: Insight into mechanisms and consequences. In *Stem Cells and Aging*; Elsevier: Amsterdam, The Netherlands, 2021; pp. 103–111. [CrossRef]
23. Liu, B.; Qu, J.; Zhang, W.; Izpisua Belmonte, J.C.; Liu, G.H. A stem cell aging framework, from mechanisms to interventions. *Cell Rep.* **2022**, *41*, 111451. [CrossRef]
24. Oh, J.; Lee, Y.D.; Wagers, A.J. Stem cell aging: Mechanisms, regulators and therapeutic opportunities. *Nat. Med.* **2014**, *20*, 870–880. [CrossRef] [PubMed]
25. Magal, P.; Ruan, S. *Theory and Applications of Abstract Semilinear Cauchy Problems*; Applied Mathematical Sciences; Springer International Publishing: Cham, Switzerland, 2018; Volume 201. [CrossRef]
26. Perthame, B. *Transport Equations in Biology*; Frontiers in Mathematics; Birkhäuser Basel: Basel, Switzerland, 2007. [CrossRef]
27. Cui, M.; Lv, Y.; Pan, H.; Yang, L. Hopf-bifurcation analysis of a stage-structured population model of cell differentiation. *Phys. D Nonlinear Phenom.* **2024**, *467*, 134266. [CrossRef]
28. Doumic, M. Analysis of a Population Model Structured by the Cells Molecular Content. *Math. Model. Nat. Phenom.* **2007**, *2*, 121–152. [CrossRef]
29. Zhang, X.; Liu, Z. Periodic oscillations in age-structured ratio-dependent predator–prey model with Michaelis–Menten type functional response. *Phys. D Nonlinear Phenom.* **2019**, *389*, 51–63. [CrossRef]
30. Webb, G.F. Population Models Structured by Age, Size, and Spatial Position. In *Structured Population Models in Biology and Epidemiology*; Lecture Notes in Mathematics; Morel, J.M., Takens, F., Teissier, B., Magal, P., Ruan, S., Eds.; Springer: Berlin/Heidelberg, Germany, 2008; Volume 1936, pp. 1–49. [CrossRef]
31. Jilkine, A. Mathematical Models of Stem Cell Differentiation and Dedifferentiation. *Curr. Stem Cell Rep.* **2019**, *5*, 66–72. [CrossRef]
32. Fischer, M.M.; Blüthgen, N. On tumoural growth and treatment under cellular dedifferentiation. *J. Theor. Biol.* **2023**, *557*, 111327. [CrossRef]
33. Wang, Y.; Zhao, J.; Park, H.J.; Zhou, D. Effect of dedifferentiation on noise propagation in cellular hierarchy. *Phys. Rev. E* **2022**, *105*, 054409. [CrossRef]
34. Wodarz, D. Effect of cellular de-differentiation on the dynamics and evolution of tissue and tumor cells in mathematical models with feedback regulation. *J. Theor. Biol.* **2018**, *448*, 86–93. [CrossRef]
35. Mahdipour-Shirayeh, A.; Kaveh, K.; Kohandel, M.; Sivaloganathan, S. Phenotypic heterogeneity in modeling cancer evolution. *PLoS ONE* **2017**, *12*, e0187000. [CrossRef]
36. Jilkine, A.; Gutenkunst, R.N. Effect of Dedifferentiation on Time to Mutation Acquisition in Stem Cell-Driven Cancers. *PLoS Comput. Biol.* **2014**, *10*, e1003481. [CrossRef]
37. Zhou, D.; Luo, Y.; Dingli, D.; Traulsen, A. The invasion of de-differentiating cancer cells into hierarchical tissues. *PLoS Comput. Biol.* **2019**, *15*, e1007167. [CrossRef]
38. Chen, X.; Wang, Y.; Feng, T.; Yi, M.; Zhang, X.; Zhou, D. The overshoot and phenotypic equilibrium in characterizing cancer dynamics of reversible phenotypic plasticity. *J. Theor. Biol.* **2016**, *390*, 40–49. [CrossRef]
39. Zhou, D.; Wang, Y.; Wu, B. A multi-phenotypic cancer model with cell plasticity. *J. Theor. Biol.* **2014**, *357*, 35–45. [CrossRef] [PubMed]
40. Zhou, D.; Wu, D.; Li, Z.; Qian, M.; Zhang, M.Q. Population dynamics of cancer cells with cell state conversions. *Quant. Biol.* **2013**, *1*, 201–208. [CrossRef] [PubMed]

41. Rhodes, A.; Hillen, T. Mathematical Modeling of the Role of Survivin on Dedifferentiation and Radioresistance in Cancer. *Bull. Math. Biol.* **2016**, *78*, 1162–1188. [CrossRef] [PubMed]
42. Wang, Y.; Lo, W.C.; Chou, C.S. Modelling stem cell ageing: A multi-compartment continuum approach. *R. Soc. Open Sci.* **2020**, *7*, 191848. [CrossRef]
43. Xia, M.; Li, X.; Chou, T. Overcompensation of transient and permanent death rate increases in age-structured models with cannibalistic interactions. *Phys. D Nonlinear Phenom.* **2024**, *470*, 134339. [CrossRef]
44. Perko, L. *Differential Equations and Dynamical Systems*; Texts in Applied Mathematics; Springer New York: New York, NY, USA, 2001; Volume 7. [CrossRef]
45. Hirsch, M.W.; Smith, H.L. Chapter 4 Monotone Dynamical Systems. In *Handbook of Differential Equations: Ordinary Differential Equations*; Elsevier: Amsterdam, The Netherlands, 2006; Volume 2, pp. 239–357. [CrossRef]
46. Ladyzhets, S.; Antel, M.; Simao, T.; Gasek, N.; Cowan, A.E.; Inaba, M. Self-limiting stem-cell niche signaling through degradation of a stem-cell receptor. *PLoS Biol.* **2020**, *18*, e3001003. [CrossRef]
47. Wang, L.S.; Yu, J. Analysis Framework for Stochastic Predator–Prey Model with Demographic Noise. *Results Appl. Math.* **2025**, *27*, 100621. [CrossRef]
48. Liu, Z.; Wang, L.S.; Yu, J.; Zhang, J.; Martel, E.; Li, S. Bidirectional Endothelial Feedback Drives Turing–Vascular Patterning and Drug-Resistance Niches: A Hybrid PDE–Agent-Based Study. *Bioengineering* **2025**, *12*, 1097. [CrossRef] [PubMed]

Disclaimer/Publisher's Note: The statements, opinions and data contained in all publications are solely those of the individual author(s) and contributor(s) and not of MDPI and/or the editor(s). MDPI and/or the editor(s) disclaim responsibility for any injury to people or property resulting from any ideas, methods, instructions or products referred to in the content.